OPTICAL QUANTUM DOT FILMS FOR WIDE COLOR GAMUT SMART PHONE DISPLAYS

A Thesis

by

Süleyman Efdal Mutcu

Submitted to the
Graduate School of Sciences and Engineering
In Partial Fulfillment of the Requirements for
the Degree of

Master of Science

in the
Department of Electrical and Electronics Engineering

Özyeğin University
May 2019

OPTICAL QUANTUM DOT FILMS FOR WIDE COLOR GAMUT SMART PHONE DISPLAYS

Approved by:

Prof. Güray Erkol
Department of Natural and Mathematical Sciences
Özyeğin University

Asst. Prof. Sedat Nizamoğlu
Department of Electrical and Electronics Engineering
Koç University

Asst. Prof. Kadir Durak
Department of Electrical and Electronics Engineering
Özyeğin University

Asst. Prof. Bora Işıldak
Department of Electrical and Electronics Engineering
Özyeğin University

Asst. Prof. Emir Salih Mağden
Department of Electrical and Electronics Engineering
Koç University

Date Approved: 08.05.2019

To my family…

ABSTRACT

Liquid crystal display (LCD) technology is a fundamental constituent of today's smart phones for image formation. LCDs are required to have a back light unit (BLU) to create a uniform white light with the correct color coordinates. Light emitting diodes (LEDs) are important building blocks as light sources in LCD-BLUs. LEDs use blue-emitting semiconductor chips and yellow-emitting phosphors on top of these chips as color converting agents. Phosphors emit radiation around 500 – 700 nm wavelength range after stimulated by blue photons and consequently white light is produced with the combination of blue and yellow dominant broad spectral emission. Color gamut value with this method yields around 70% in National Television System Committee (NTSC) standards and causes mediocre color quality for the displays in color space defined by International Commission on Illumination (CIE). Quantum dots (QDs) have high capacity to satisfy the rapidly increasing demands for display panels that require high color quality and range. Their size-tunable optical properties and high quantum efficiency make QDs as desirable substitutes to phosphors. This thesis includes the synthesis of green- and red-emitting QD nanocrystals and preparation of color converting optical films using optically transparent polydimethylsiloxane (PDMS) polymers with the aim of increasing the color gamut of smart phone displays. The prepared color converting films were optimized to be compatible with the smart phone BLU. The spectral measurements yielded 95% NTSC color gamut value. In this study, QD polymeric film application was applied to the smart phone displays for the first time and a 35% increase in color gamut was observed.

ÖZET

Sıvı kristal ekran teknolojisi kullanan akıllı telefonlarda görüntünün oluşturulabilmesi için arka-ışık üniteleri ve bu arka ışık ünitelerinde ışık kaynağı olarak ışık yayan diyotlar kullanılmaktadır. Işık yayan diyotlar mavi renkte ışıma yapan çiplere sahiptir ve bu çiplerin üzerinde çeşitli oranlarda kaplanmış fosfor atomları bulunmaktadır. Mavi ışık aracılığıyla uyarılan fosfor atomları, görünür bölge spektrumunda 500-700 nm dalga boylarında ışıma yaparlar ve tüm bu ışımaların birleşimi ile beyaz ışık üretilmiş olur. Bu yöntemle üretilen beyaz ışığın renk gamı değeri ise yaklaşık olarak %70 NTSC seviyelerindedir. Bu da ekrandan elde edilen renk kalitesinin insan gözünün görebileceği renk uzayına kıyasla düşük olmasına sebep olmaktadır. Tez çalışmaları kapsamında ekran renk gamının artırılması için kırmızı ve yeşil renkte ışıma yapan kuantum nokta nanoparçacıklar sentezlenmiş ve sentezlenen bu parçacıklar optik geçirgen PDMS polimeri kullanılarak renk dönüştürücü optik film olarak hazırlanmıştır. Hazırlanan renk dönüştürücü filmler akıllı telefon arka ışık ünitesine uyumlu olacak şekilde optimize edilmiş, arka ışık ünitesi mekanik yapısına uygun şekilde tasarlanan ve mavi renkte ışıyan ışık barı ile uyarılarak yüksek renk gamına sahip beyaz ışık elde edilmiştir. Oluşturulan sistemin spektroradyometre aracılığı ile optik ölçümleri yapılmış ve yapılan hesaplamalar ile birlikte %95 NTSC renk gamı elde edilmiştir. Kuantum nokta optik film uygulaması ilk defa akıllı telefon ekranlarına uyarlanmış ve %35 oranında renk iyileştirmesi sağlanmıştır.

ACKNOWLEDGMENTS

I express my sincere respect and gratitude to my advisers Asst. Prof. Sedat Nizamoğlu and Prof. Güray Erkol for their support and guidance.

I would like to thank Dr. Sadra Sadeghi for his bright ideas during quantum dot nanocrystal synthesis and his marvelous support. I would also like to thank Mr. Kıvanç Karslı for his guidance in the face of difficulties with his motivational approach and technical background.

I would like to express my gratitude to Dr. Güneş Aydındoğan for his invaluable support during all of my thesis studies. I would also like to thank him for his sincere patience and humble approach during the experiments.

Once and for all, I am grateful to my priceless mother and my family, who are the biggest power source behind my success.

TABLE OF CONTENTS

I ABSTRACT iv

II ÖZET v

III ACKNOWLEDGMENTS vi

IV TABLE OF CONTENTS vii

V LIST OF FIGURES ix

VI LIST OF TABLES xii

VII INTRODUCTION 1

VIII SCIENTIFIC BACKGROUND 4

2.1 Human Color Vision and Color Science 4

2.2 Liquid Crystal Display Systems 10

2.3 Backlight Units 11

2.3.1 Light Emitting Diodes 12

2.3.2 Light Guide Plate 14

2.3.3 Optical Films 15

2.4 Color-Converting Nanocrystal Quantum Dots 17

IX METHODOLOGY 21

3.1 Quantum Dot Nanocrystal Synthesis 21

3.1.1 Red-Emitting CdSe/CdS Quantum Dot Synthesis 21

3.1.2 Red-Emitting CdSe/ZnS Quantum Dot Synthesis 22

3.1.3 Green-Emitting CdSe/ZnS Quantum Dot Synthesis 23

3.2 Optical Film Fabrication 24

X MEASUREMENTS and RESULTS 29

4.1 Smartphone Backlight Unit 29

4.1.1 Optical Structure of Backlight Unit 30

4.2 Color Filter Measurements of the LCD 30

4.3 Quantum Dot Measurements 34

4.3.1 Quantum Dot Photoluminescence Measurements 34

4.3.2 Red-Emitting Quantum Dot Photoluminescence Measurements35

4.3.3 Green-Emitting Quantum Dot Photoluminescence Measurements 36

4.4 Quantum Dot Film Measurements 37

4.4.1 Optical Analysis of Produced QD Films 37

4.4.2 Red-Emitting CdSe/CdS & Green-Emitting CdSe/ZnS QD Film Measurements at LCD Panel.....39

4.4.3 Red-Emitting CdSe/ZnS & Green-Emitting CdSe/ZnS QD Film Measurements at LCD Panel.....40

4.5 Discussion 42

XI CONCLUSION.....45

XII BIBLIOGRAPHY 46

XIII VITA 50

LIST OF FIGURES

Figure 1: Schematic presentation of the human eye and enlarged view of the retina.....4

Figure 2: Spectral sensitivity distribution of rod and cone cells.....5

Figure 3: Standard observer color matching functions. 6

Figure 4: The CIE 1931 color space chromaticity diagram.....7

Figure 5: Planckian Locus in the CIE 1931 chromaticity diagram.....8

Figure 6: NTSC Color Gamut on CIE 1931 Color Space. 9

Figure 7: Schematic edge-lit BLU and LCD structure.....11

Figure 8: Schematic representation of a typical GaN LED chip.....12

Figure 9: Different types of LED applications. 13

Figure 10: Schematic working principle of patterned LGPs. 14

Figure 11: Top view of dot-patterned LGP. 15

Figure 12: Schematic representation of diffuser films. 16

Figure 13: Schematic representation of prism films. 16

Figure 14: Schematic representation of reflector films. 17

Figure 15: Formal illustration of a core/shell structured quantum dot (left) and energy band diagram (right). 18

Figure 16: Size dependent emission spectrum of CdSe QDs (left) and the absorption spectrum of CdSe QDs (right). 19

Figure 17: The appearance of the post-synthesis green solution under UV 23

Figure 18: Red and green QD nanocrystals dissolved in Hexane under UV.....24

Figure 19: Mixed QD solutions in petri dishes. (left) Green-emitting QD solution and (right) red-emitting QD solution. 25

Figure 20: Mixed QDs solutions at vacuum chamber. 26

Figure 21: Vacuum table when the vacuuming is (left) off and (right) on. 26

Figure 22: Pouring of the mixture with an injection syringe. 27
Figure 23: Dr. Blade application. 27
Figure 24: Prepared green- and red-emitted QD films under 365nm UV irradiation. 28
Figure 25: Smartphone BLU (left) off and (right) on. 29
Figure 26: Designed LED Bar 2D drawing. 30
Figure 27: Schematic optical structure of the BLU. 30
Figure 28: Spectroradiometer. 31
Figure 29: RGB spectral output of the white illuminated LCD. 32
Figure 30: Spectral output of the BLU. 32
Figure 31: Transmittance characteristics of the RGB CFA. 33
Figure 32: Spectroflourometer 34
Figure 33: Emission measurement of red-emitting QDs. 35
Figure 34: Absorption measurement of red-emitting QDs. 35
Figure 35: Emission measurement of green-emitting QDs. 36
Figure 36: Absorption measurement of green-emitting QDs. 36
Figure 37: Structural optical film combination of BLU. 37
Figure 38: Produced red- and- green-emitting QD films with different thicknesses 38
Figure 39: The optical intensity output of the fabricated red- and green-emitting films with different thicknesses when excited by blue source 38
Figure 40: Spectrum output of the red-emitting CdSe/CdS and green-emitting CdSe/ZnS QD films in the BLU. 39
Figure 41: Color gamut triangle of the red-emitting CdSe/CdS and green-emitting CdSe/ZnS QD films in the LCD. 40
Figure 42: Spectrum output of the red-emitting CdSe/ZnS and green-emitting CdSe/ZnS QD films in the BLU. 41

Figure 43: Color gamut triangle of the red-emitting CdSe/ZnS and green-emitting CdSe/ZnS QD films in the LCD. 42
Figure 44: Schematic improvement in the color gamut triangle.....43
Figure 45: Color quality difference of the produced displays. (left) Commercial product contains standard white LED in BLU, (right) QD film embedded product. 43

LIST OF TABLES

Table 1: Cx, Cy and luminance values of BLU and WRGB measurements. 33

Table 2: Optical outputs of red-emitting CdSe/CdS and green-emitting CdSe/ZnS QD films in the LCD. 40

Table 3**:** Optical outputs of red-emitting CdSe/ZnS and green-emitting CdSe/ZnS QD films in the LCD. 41

CHAPTER I

INTRODUCTION

In the last decades, thin-film-transistor liquid-crystal-displays (TFT-LCDs) have been positioned at the top of imaging technologies as flat panel displays with increasing sales quantities all over the world [1]. Users can interact with visual contents through LCDs; though it plays the most important role in display systems on a wide scale ranging from computer screens to televisions (TVs), smartphones, and tablets. Due to the technological developments, imaging quality parameters such as viewing angle, contrast level or response time of pixels have been improved by TFT-LCD producers so far, placing LCDs at an indispensable position at the market [2]. Although the rapid increase of organic light-emitting diode (OLED) displays creates a compelling challenge, it contributes to gradual development of LCDs as well.

In order to create an image in LCD systems, the color filter arrays (CFAs) located in each pixel should be illuminated by light in the visible range of the electromagnetic spectrum. The number of pixels varies according to the resolution capacity. The light passing through each pixel is produced in the BLUs of the LCD panels, and the characteristics of the light sources used in these BLUs are the factors that determine the quality of the image, i.e., luminance, color coordinates, and color gamut obtained from the screen.

At the beginning of LCD technology, cold cathode fluorescent lamps (CCFL) were used in backlight units as light sources. However, since CCFLs consume high energy and do not allow thin screen design, the entire display market quickly switched to use LEDs as light sources at BLUs [3].

The first attempt to use LEDs as light sources was multi-LED-chip approach which

contains red, green, and blue emitters. These kinds of LEDs generate white light by mixing the three primary colors. Despite their wide usage in lightning applications, this method leads researchers for cost efficient alternatives, one of which is to use an ultraviolet (UV) LED chip with a phosphor that converts the UV to white light. Considering the low light conversion efficiency of this method, a third approach presented itself. A yellow phosphor on top of a blue LED chip is now the most conventional method in the literature thanks to its higher light conversion and cost efficiency.

QDs are emissive semiconducting materials that have the advantage of high efficiency, narrow emission band, and spectral tunability. These nanoscale crystals have size-dependent optical properties which can be applied to different branches of technology ranging from display products to biomedical applications. Their unique properties in the visible range of the spectrum and the comparative advantages in display panels as color convertors encourage researchers to focus on colloidal QD synthesis and control their optical features [4].

QDs can be synthesized by either wet chemical methods or dry methods which are called colloidal and epitaxial, respectively. Epitaxial methods require high energy input, and possess weak quantum-confinement effects whereas colloidal synthesis has many advantages over their epitaxial counterpart such as size control, spectral purity and photoluminescence quantum yield. Another important feature of colloidal QDs is their organic ligand dressings that enable QDs to couple with different polymers which are a crucial factor in this research. Therefore colloidal QDs are preferred in the subsequent sections and referred simply as QDs.

In this thesis study, optical properties of QD nanocrystals were investigated experimentally as an optical component in wide color gamut display panels. A brief

scientific background about QDs and display panels are given in Chapter 2 along with definitions of display metrics such as color space, chromaticity coordinates, color temperature, and color gamut. In Chapter 3, the synthesis methods, polymerization steps, and film preparation process are explained in detail followed by measurement setup, results and a comprehensive discussion in Chapter 4.

CHAPTER II

SCIENTIFIC BACKGROUND

2.1 Human Color Vision and Color Science

The human eye is equipped with sensors with different spectral properties to create our sight orbit that enables us to evaluate our surroundings. This includes the interpretation of the colors that are produced by a light source, which requires standardization amongst the researchers, therefore color science is introduced to have a quantitative criterion for the lightning and display related products. For this reason, understanding the vision of the human eye plays a vital role in the design of the display systems.

The outer layer of the human eye, also known as the cornea, is made of a molecular structure that allows it to be completely transparent. The light reflected from the objects initially passes through the cornea then reaches the part which is filled with a completely transparent liquid called the anterior chamber. The fluid pressure in this section is controlled by the eye ball, and the incoming light waves fall on the lens for focus after passing through the liquid [5]. Schematic representation of the eye is shown in Fig. 1.

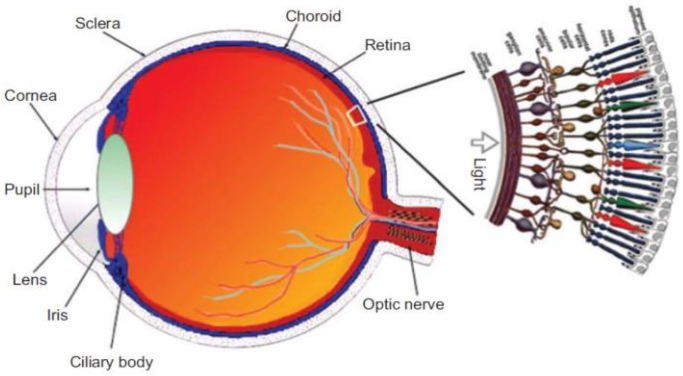

Figure 1: Schematic presentation of the human eye and enlarged view of the retina [6].

The light rays focused by the lens are directed to the layer called retina which has three layers called photoreceptors, neurons and fibers. Photoreceptors are directly proportional to light sensitivity via rods and cones. Rod cells are responsive to the entire visible spectrum and allow us to see them especially in low light conditions. However, these cells do not play any major role in distinguishing the colors. The cells that enable us to see and distinguish colors are cone cells that are specialized for three primary colors which are red, green and blue [7]. The spectral sensitivity distribution of these cells is shown in Fig. 2.

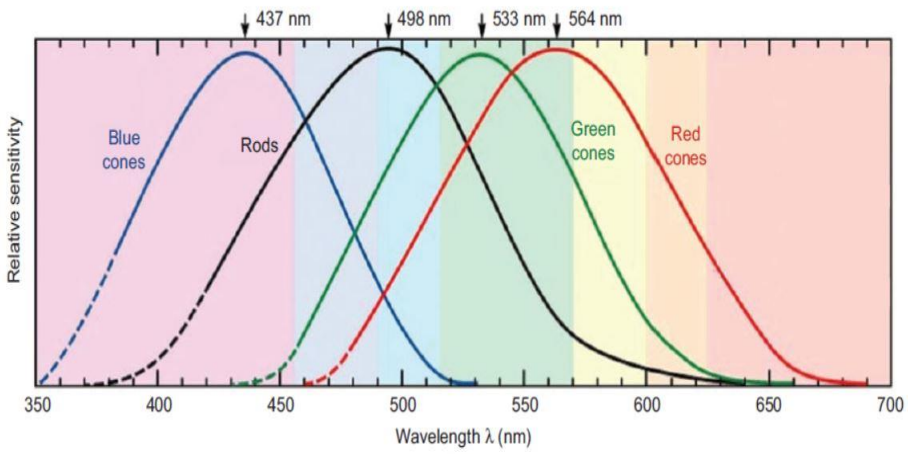

Figure 2: Spectral sensitivity distribution of rod and cone cells [7].

International Commission for Illumination (Commission Internationale de l'Eclairage, CIE) has defined color matching functions for these three primary colors based on their sensitivity spectrum as x, y and z, respectively. Color matching functions describe the chromatic response of the observer whose spectral distribution is shown in Fig. 3.

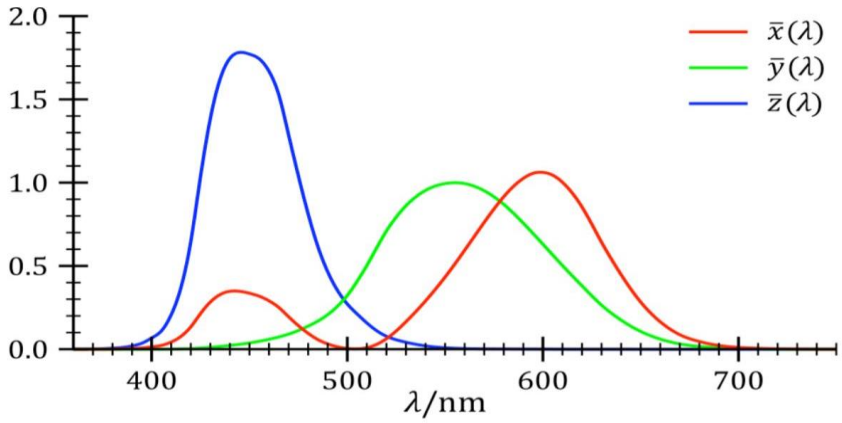

Figure 3: Standard observer color matching functions [8].

Color matching functions can be considered as spectral sensitivity curves of linear light sensing elements for the CIE tristimulus values X, Y and Z. Tristimulus values can be defined as in the following formulas that include spectral radiance of any color [9]:

$$X = \int_{380}^{780} L_\lambda \bar{x}_\lambda d\lambda \tag{1}$$

$$Y = \int_{380}^{780} L_\lambda \bar{y}_\lambda d\lambda \tag{2}$$

$$Z = \int_{380}^{780} L_\lambda \bar{z}_\lambda d\lambda \tag{3}$$

Where λ is the wavelength of the equivalent monochromatic light and L_λ is radiance spectrum. The chromaticity coordinates can be calculated by using the following equations.

$$x = \frac{X}{X+Y+Z} \tag{4}$$

$$y = \frac{Y}{X+Y+Z} \tag{5}$$

$$z = \frac{Z}{X+Y+Z} \tag{6}$$

These chromaticity coordinates can be mapped onto a two-dimensional diagram to visualize the color space. Hence, the chromaticity diagram of CIE 1931 is formed by using the color matching functions and chromaticity coordinate equations. The horseshoe shaped color space is illustrated in Fig. 4.

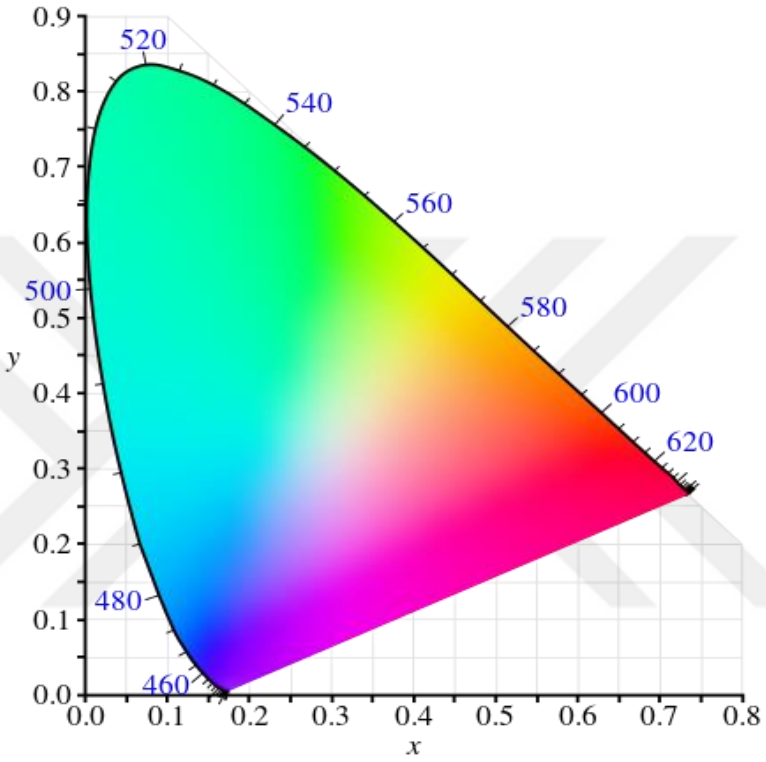

Figure 4: The CIE 1931 color space chromaticity diagram [8].

Lightning systems and display products need to be designed such that their spectral output matches the human eye sensitivity function that has a peak at 550 nm, since the overlapping ratio of the two functions directly affects the color quality of the product.

Color temperature is another display metric defined on the CIE color space that depicts the shade of the white light. The black body radiation experiments reveal the chromaticity coordinates of the black body radiators at different temperatures under the

name of Planckian Locus (see Fig. 5). In this way, temperatures of the blackbody radiators associated with any coordinate on the Planckian Locus can be defined as the color temperature of the white light source that has the same coordinates.

If the coordinates of the light source do not fall onto the Planckian Locus, then the chromaticity coordinates of the blackbody radiator close to that of the white light source can be taken as the color temperature. In this case, the temperature of the light source is referred as correlated color temperature (CCT).

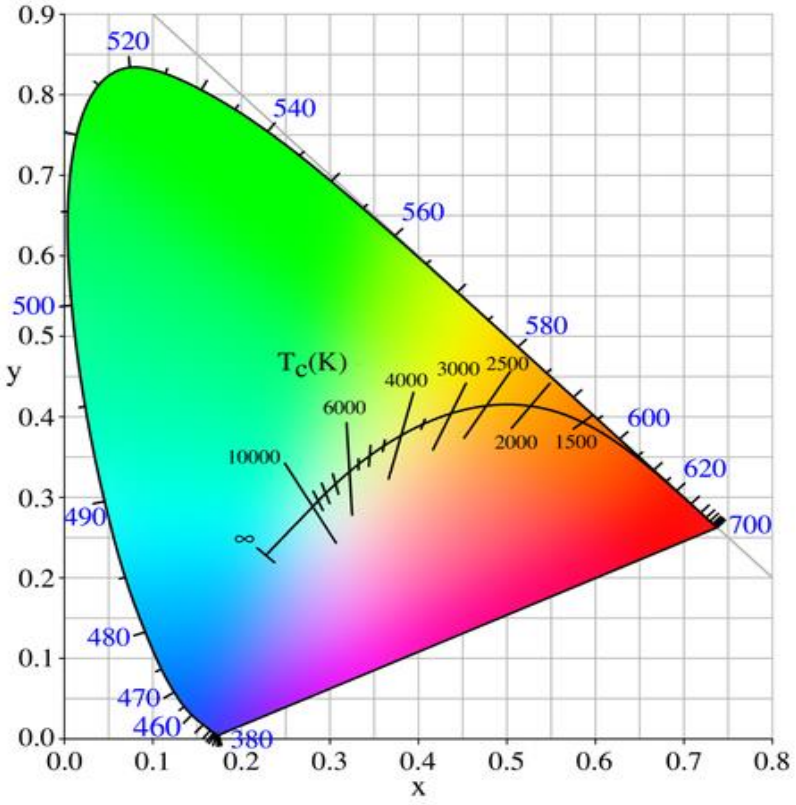

Figure 5: Planckian Locus in the CIE 1931 chromaticity diagram [8].

Each white light source is defined according to their CCT values and they are customized according to their areas of usage. Incandescent light sources are in the 3000K zone defined as warm white, whereas fluorescent and white LED light sources are in the 6500K zone defined as cold white according to their CCT values [7].

The radiometric and photometric properties of human vision system should be defined considering the radiance and luminance parameters. The radiance is the radiometric number indicating the optical power per solid angle per unit area and defined by $W_{opt}/(m^2 sr)$.

The luminance function is described by using spectral radiance and human eye sensitivity function as

$$L = 683 \frac{lm}{W_{opt}} \int P_L(\lambda) V(\lambda) d\lambda \tag{7}$$

The final display metric that will be introduced in this thesis work is the color gamut, which is the triangle formed by the red, green and blue color coordinates obtained by the chromaticity measurements of the light sources. The color gamut triangle that was defined by the National Television System Committee (NTSC) in 1953 is shown in the Fig. 6.

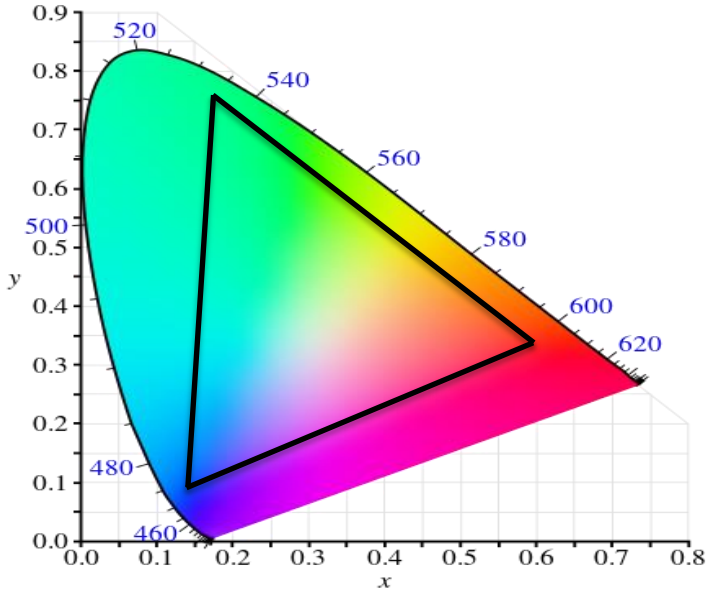

Figure 6: NTSC Color Gamut on CIE 1931 Color Space.

The area within the triangle covers all the colors that any display system can show to the users. All display systems define their color gamut according to NTSC standards. With the advances in technology, new standards which correspond to larger color gamut values have been defined such as sRGB, DCI-P3, or Rec2020. The color gamut values along with the chromaticity coordinates are of great importance in determining the color quality of display technologies.

2.2 Liquid Crystal Display Systems

The role of imaging technologies in shaping the modern world is confronted with an undeniable reality [10]. With the advances in technology, the tremendous increase in the color quality offered to the end users has led the researchers and manufacturers to further invest in display technologies in recent years. The technological advancements in material science, developments in advanced production techniques and advance software algorithms have substantial contributions to current TFT-LCD technologies. Thus, LCD technologies are positioned at top of the display systems like TVs, monitors, tablets and smartphones with the advantages of production cost, lifetime, color quality and reliability [11].

LCD technologies need a BLU to create the image since there is no light-emitting material to illuminate the display panel in the conventional structure of the LCs. In today's technology, the BLUs usually use white LEDs as light source and various optical films to manipulate the direction and the intensity of light. BLUs can be classified as direct-lit (DLED) and edge-lit (ELED) displays, according to the position of the light source. In DLED panels, LEDs are positioned opposite to the LC cell. The uniform distribution of light and cloaking of the LEDs are achieved by the intermediate optical films; e.g., diffuser plate, diffuser sheet, prism sheet, brightness enhancement

film. Despite the cost effectiveness of the DLED panels compared to the ELEDs, the distance between the LEDs and the LC cell need to be long enough (between 15 – 40 mm), which causes a thicker structure than ELEDs. Hence, DLED-type BLUs are not preferred in smart phone applications. On the other hand, LEDs are located at one or two edges of the panel in edge-lit BLUs. The distribution of light are provided via a light guide plate (LGP) instead of a diffuser plate. The other optical films are similar with that of DLEDs. Schematic edge-lit BLU and LCD structure can be seen in Fig. 7.

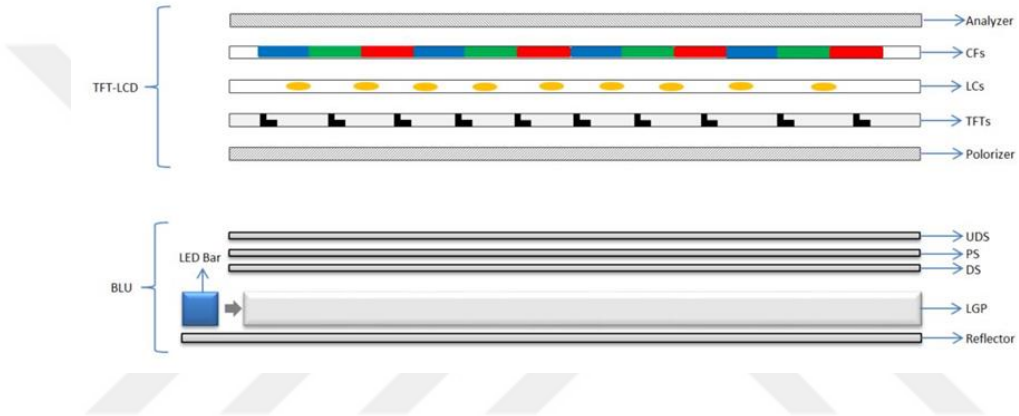

Figure 7: Schematic edge-lit BLU and LCD structure.

In Fig. 7, the light produced from the LED bar is directed vertically through the LGP to other optical components and the luminance intensity with these structure is enhanced.. The increased luminous flux loses a significant portion of its intensity when it passes through the first polarizer [12]. Polarized light is sent to CFs via LCs and TFTs according to content signals from TFT driver, then simultaneous illumination of all cells creates image on the screen.

2.3 Backlight Units

BLUs are vital for liquid crystal display technologies as they provide the light source that leads the formation of colors and include various optical components like LEDs,

LGPs and several optical sheets as shown in Fig. 7. Although CCFLs were used as a light source for LCDs in previous years, due to their high efficiency, long lifetime and low costs, phosphorus converted white LEDs are used in BLU structures as the most preferred light sources today [13, 14]. The BLUs are divided into two groups as direct-lit and edge-lit according to their position in the optical structure. Smartphones are consequently equipped with the edge-lit BLU structure because of their thin mechanical structures.

2.3.1 Light Emitting Diodes

LEDs are semiconductor devices that have p-n junction structures which radiate when a driving voltage is applied. In the most basic sense, the electrons in the transmission band of the n-junction and the holes in the valence band of the p-junction flow to each other with the applied voltage and form recombination. This recombination energy is equal to the energy of the oscillating photon and the energy gap between the conduction and the valence bands [15].

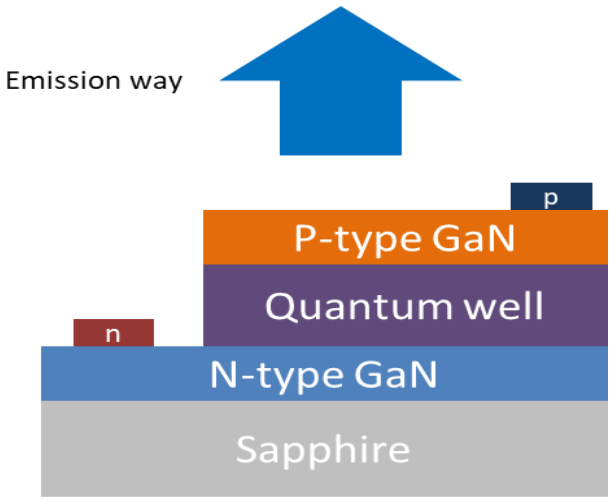

Figure 8: Schematic representation of a typical GaN LED chip.

The photon emission wavelength depends on the types and thicknesses of each layer within the structure, and it can be formed in different types for various applications. Nowadays, LED chips are mostly formed with GaN structure and they are radiating at the blue region of the visible spectrum.

White LEDs used in BLUs are manufactured in various ways. Nowadays, the most anticipated method is to coat the yellow phosphor material onto the blue chip. In this way, the blue photons incident from the chip stimulates the phosphorous atoms in order to obtain higher wavelength radiations to create white light. With this method, the stimulated phosphorus atoms radiate at the green and red areas of the visible spectrum with a wide full-width half-maximum (FWHM) value. The different types of LED applications used to create white light are shown in Fig. 9.

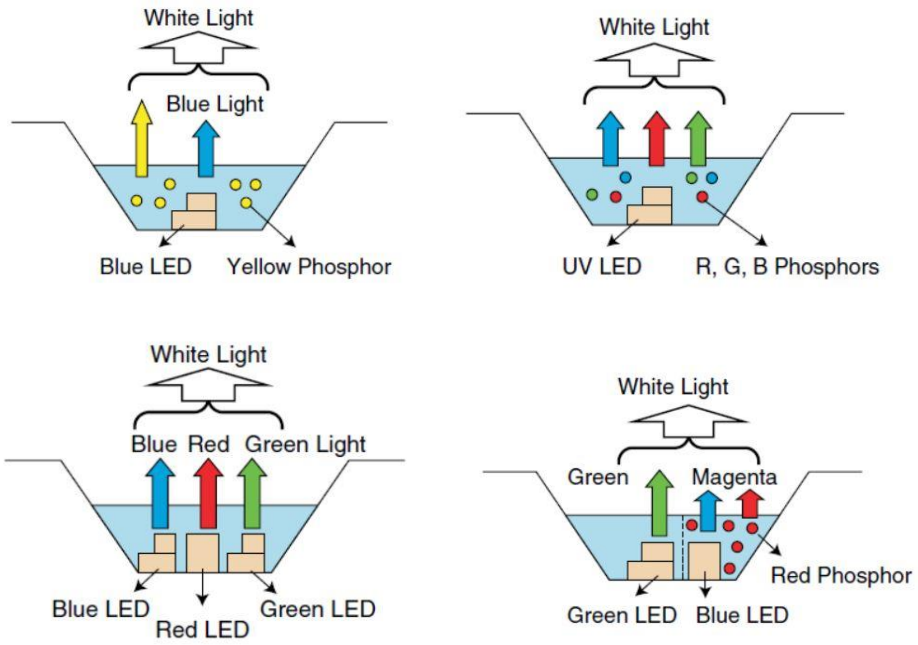

Figure 9: Different types of LED applications [15].

The color gamut of white light obtained from yellow phosphor coated LEDs are lower than that of the RGB phosphorus coated LEDs. One of the main reasons is that the radiation bandwidth obtained in the green and red regions is wider in the first case

and the other is that the peak wavelength of the radiation in the red zone is around 600nm, which should ideally be around 620 nm.

2.3.2 Light Guide Plate

In edge-lit BLUs, photons coming from the light source must be spread uniformly on the entire screen surface and directed to the TFT-LCD. LGPs undertake the task of redirecting the light towards the optical films and LCD through its patterns located at the bottom surface. Incident rays enter the LGP from one of the side surfaces of the structure and change their orientation by scattering on the reflective patterns on the bottom surface.

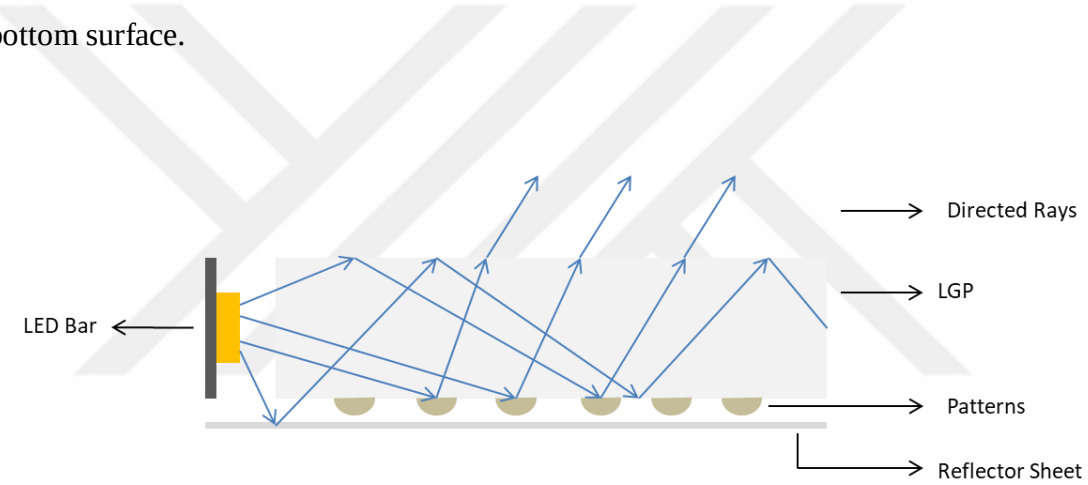

Figure 10: Schematic working principle of patterned LGPs.

LGPs are usually made from transparent materials such as polymethylmethacrylate (PMMA), polycarbonate (PC) or glass. Reflective patterns in the lower surface of LGP are formed by masking method with high-reflectivity materials. In addition to the masking methods, the designed patterns can be formed on the LGP bottom surface by a method called hot roll stamping. The distribution of the patterns on the LGP surface is determined using various optical design and simulation programs.

The optical performance simulations can be constructed upon the optical modelling of the BLU, and then a ray tracing technique is employed to predict the

behavior of light rays. Basically, fundamental properties of dot patterns such as their position and size can be optimized with the simulation tool to fulfill the specifications. Since it is not applicable to change the position and size of the dots, LGP production can only be made once the locations and the dimensions of the dots are determined. There is a feedback mechanism between the simulation results and the manufactured samples in the design verification process. After the optical measurements of the produced LGPs which are evaluated, the design is reviewed according to the correlation between the measurement results and the target luminance and light distribution. This cycle continues until sufficient uniformity and luminance results are captured over the entire area of the LGP [16]. Top view of an LGP with dot patterns is shown in Fig. 11.

Figure 11: Top view of dot-patterned LGP.

2.3.3 Optical Films

Polymeric optical films with different optical properties are used in BLUs to diffuse, collimate, or redirect light. The most basic feature of these films is to manipulate the light rays obtained from the light source (LEDs) towards the TFT-LCD structure with the highest possible intensity and optimal distribution. In the BLUs, three different types of optical films are used, which has mainly reflective, diffusive and enhancive properties.

In general applications, diffuser films are used to homogenously distribute light rays that are coming from the LPG to the display surface. In Fig. 12, the distribution irregularities of the light on the screen are reduced by the micro-beads used on the diffuser film surface.

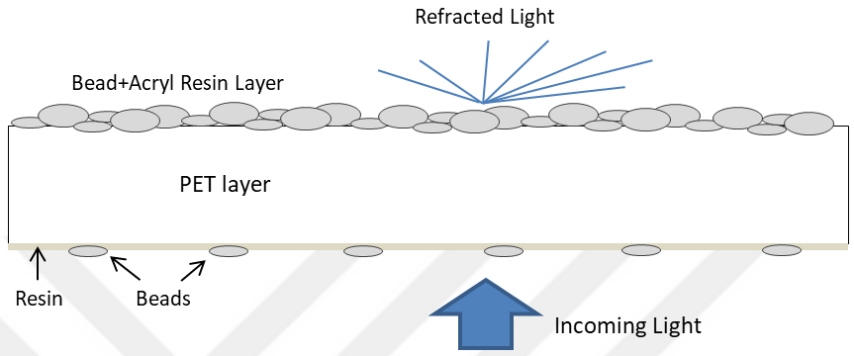

Figure 12: Schematic representation of diffuser films.

Prism films are one of the most basic optical components used to increase the brightness of light passing through LGP and diffuser films due to their enhancive properties [17]. These components play a vital role in increasing the total luminescence by directing the light from the bottom surface towards the user direction via periodic micro-prismatic structures on their surface as shown in Fig. 13.

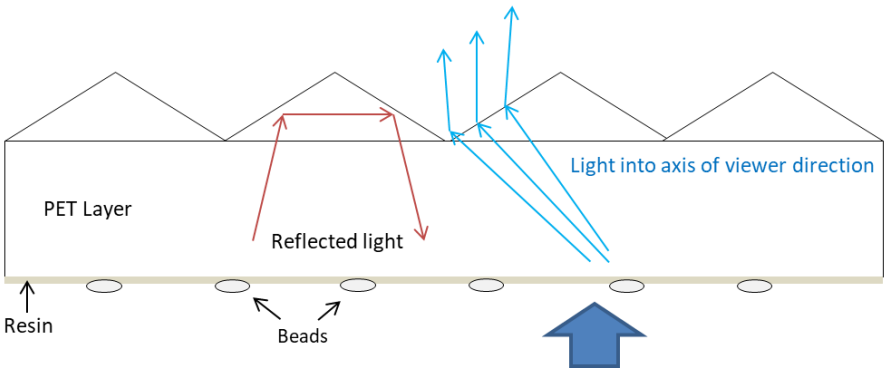

Figure 13: Schematic representation of prism films.

Reflector films are used to recover the light from internal and reverse reflections on the lower surface of LGP. It plays an important role in the recovery of light losses within the whole BLU system as shown in Fig. 14.

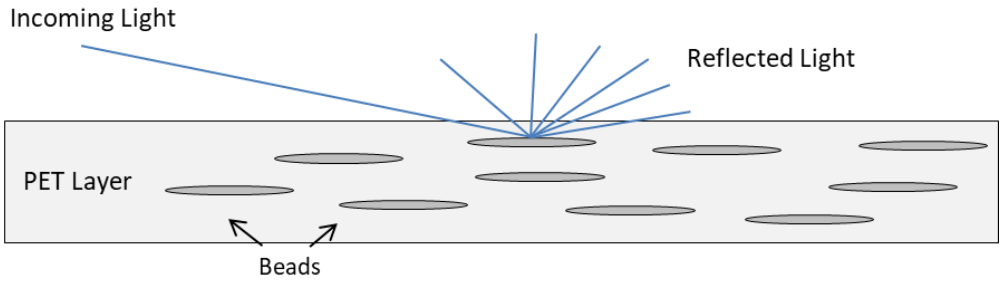

Figure 14: Schematic representation of reflector films.

2.4 Color-Converting Nanocrystal Quantum Dots

In recent years, advances in semiconductor technology have caused significant changes in our daily life. Intensive research on the nanoscale has allowed us to focus more on quantum mechanical device productions. From this perspective, QD nanocrystals have started to take place in a wide range from medical imaging systems to lighting products, display technologies to solar systems due to their quantum mechanical properties. The optical properties of colloidal nanocrystal QDs allow for a wide range of spectral customization through their ability of size control. The fact that the optical properties of the QDs can be customized in the visible region has enabled them to take a very important position in the display technologies [18].

When the working principle of the QDs is examined, it is observed that the electron and holes are confined between 2-10 mm in three-dimensional space typically and finite quantum effects are formed in this range [19]. Quantum well

approaches are fully observable due to the confinement of electrons and holes in this free space and the determination of well widths while their synthesis. This also transforms continuous energy levels of the nanomaterials into discrete energy levels. Formal illustration of a core/shell structured quantum dot is given below in Figure 15 with the equated energy band diagram.

Figure 15: Formal illustration of a core/shell structured quantum dot (left) and energy band diagram (right).

In terms of quantum effects, the most striking part of QD particles is that they emit photons associated with their particle radius when exposed to a photonic stimulation in the absorption zone. When the radius of the particles decreases, the emission peak wavelength moves to higher frequencies and to shorter wavelengths. The emission and absorption outputs of the particles can be directly correlated with the radii of the particles. With this principle, the desired spectral outputs of the QDs can be tuned during the synthesis of the particles. Typical spectral emission and absorption outputs of the CdSe QDs can be seen in Fig. 16.

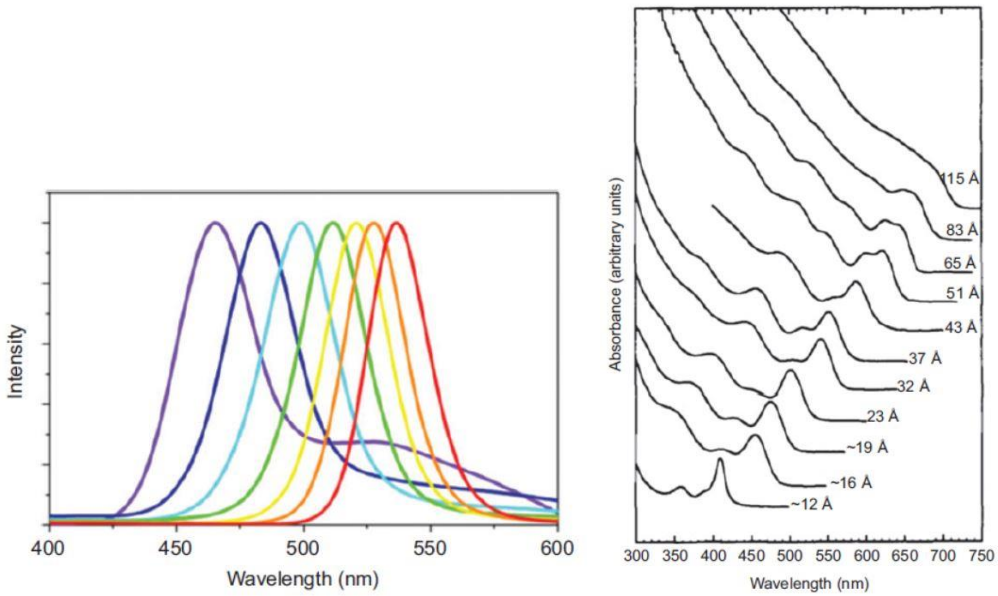

Figure 16: Size dependent emission spectra of CdSe QDs [20] (left) and the absorption spectra of CdSe QDs [21] (right).

Another remarkable feature of QD nanocrystals is that they can be produced by inexpensive chemical synthesis methods like wet chemical techniques. Ligand structures that encapsulate particles to form a potential barrier can also be bound to particles during chemical synthesis in different concepts according to their application. Although these structures differ according to the synthesis methods, they may show organic or inorganic properties. All these structural formations can be controlled by changes in the parameters such as synthesis temperature and synthesis time during the synthesis of the QDs. Depending on the synthesis method; the resulting particles are soluble in polar and non-polar solvents such as water, hexane, toluene and chloroform. Another method of synthesis is epitaxial growth and not included in this study.

When the core QD structures are synthesized alone they generally lead low quantum efficiency. Quantum efficiency of the particles are known as emitted number of photons per absorbed photon. In order to increase quantum efficiency of

the QDs, core/shell crystal structure is preferred. Thus, lattice mismatches are prevented by wrapping a structure core with a higher bandgap [22]. At present, QD structures such as CdSe/CdS, CdSe/CdS/ZnS, CdSe/ZnS, PbSe/PbS, CdTe/CdSe, CdSe/ZnTe can be synthesized over 70% quantum efficiency [23].

CHAPTER III

METHODOLOGY

3.1 Quantum Dot Nanocrystal Synthesis

In order to create any wide color gamut display using QDs, it is necessary to combine red- and green-emitting particles with blue light source. For this purpose, red- and green-emitting QD particles were synthesized based on the formation of CdSe core with gradient shell of CdS and ZnS structures separately. Gradient shells provide lower lattice mismatch between CdSe and ZnS at the core and shell interfaces to create better surface passivation and quantum efficiency [24, 25].

The methods explained in the following sections are taken from our paper "High quality quantum dots polymeric films converters for smart phone display technology" published at “Material Research Express, volume 6, number 3, 2018”.

3.1.1 Red-Emitting CdSe/CdS Quantum Dot Synthesis

CdSe/CdS red-emitting quantum dots were synthesized based on the Jang method et al [26]. In the beginning, 0.4 mmol cadmium oxide (0.0515 g, > 99.99 % Aldrich), 1.6 mmol oleic acid (0.5 ml, 99% Alfa) and 5 ml tri-n-otylamine (>97% TCI) were mixed all together in a three-neck round bottom flask which has 100 ml volume. This mixed solution was gradually heated to 150 °C under nitrogen gas flow. By keeping this temperature, the mixed solution was drained by vacuum and located under nitrogen gas flow over again. When the degassing process over, the mixed solution was heated to 300 °C. When temperature balance is achieved, dissolved 0.05 ml of 0.792 g selenium (>99.5% Aldrich) in trioctylphosphine (90% Acros) precursor (2M TOPSe) was injected into the heated solution. 2 minutes later, 1.5 ml of 210 µl 1-octanethiol

(>98.5% Aldrich) in 6 ml TOA precursor was injected into the solution gradually in 90 seconds. The mixed solution was kept under 300 °C for 40 min until the all reaction was complete.

When the reaction is over, all solution was cooled down to 20 °C for purification. At this stage, all solution was separated six centrifugal tubes and each tube filled with ethanol. Then, all tubes were centrifuged at 5000 rpm for 5 minutes and QD nanocrystals were dissociated out of solution and plastered to the edges of every tube. Finally, purificated nanocrystals dissolved again using with 2 ml hexane and all are collected in one single tube.

3.1.2 Red-Emitting CdSe/ZnS Quantum Dot Synthesis

CdSe/ZnS red-emitting quantum dots were synthesized with chemical-composition gradient method [27]. In the beginning, 0.4 mmol of CdO (0.052 g) and 4 mmol of $Zn(acetate)_2$ (0.88 g,>99.0% Sigma-Aldrich) were mixed with 17.6 mmol of oleic acid (OA) (5 ml) in a 100 ml flask. Mixed solution was heated to 150 °C, and degassed for 30 min. When the degassing is over, 15 ml of 1-octadecene (95% Sigma-Aldrich) was injected into the reaction flask and heated up to 300 °C. Reaction vessel was retained under nitrogen inert atmosphere, yielding a clear solution of $Cd(OA)_2$ and $Zn(OA)_2$.

Simultaneously, 1 mmol of Se (0.080 g) and 2.3 mmol of S (0.074 g, Reagent grade 100 mesh particle size, Sigma-Aldrich) dissolved in 3 ml of trioctylphosphine was rapidly injected into the vessel containing $Cd(OA)_2$ and $Zn(OA)_2$ at the elevated temperature of 320 °C.

In order to form the CdSe/ZnS QDs with a chemical-composition gradient, the reaction proceeded at 320 °C for 20 min. When the reaction was finished, the temperature of the reaction was lowered to room temperature. Then, purification procedures followed (dispersing in hexane, precipitating with excess acetone, repeating

three times). The resulting QDs were then dispersed in Hexane for the experiments.

3.1.3 Green-Emitting CdSe/ZnS Quantum Dot Synthesis

CdSe/ZnS green-emitting quantum dots were synthesized with chemical composition gradients by previously reported method [28]. In the beginning, 0.2 mmol of CdO (0.026 g) and 0.4 mmol of Zn (acetate)$_2$ (0.088 g, >99.0% Sigma-Aldrich) were placed with 1.6 mmol of oleic acid (OA) (0.5 ml) in a 100 mL flask. Solution was heated to 150 °C for dissolution, and degassed for 30 minutes. When the degassing is over, 15 mL of 1-octadecene (95% Sigma-Aldrich) was injected into the reaction flask and heated to 300 °C as the reaction vessel was maintained under N_2, yielding a clear solution of $Cd(OA)_2$ and $Zn(OA)_2$.

Figure 17: The appearance of the post-synthesis green solution under UV

Simultaneously, 0.2 mmol of Se (0.016 g) and 4 mmol of S (0.128 g, Reagent grade 100 mesh particle size, Sigma-Aldrich) dissolved in 2 mL of trioctylphosphine and at the elevated temperature of 300 °C, solution was rapidly injected into the vessel containing $Cd(OA)_2$ and $Zn(OA)_2$. Mixing and the reaction were proceeded at 300 °C

for 10 min in order to form the CdSe/ZnS QDs with a chemical-composition gradient.

10 minutes later, 0.5 mL of 1-octanethiol was added in the reactor to passivate the surfaces of the QDs with strongly binding ligands, than, the temperature of the reactor was cooled down to room temperature. When the synthesis is over, purification procedures followed similarly with red QDs, The resulting QDs were then dispersed hexane for optical film production.

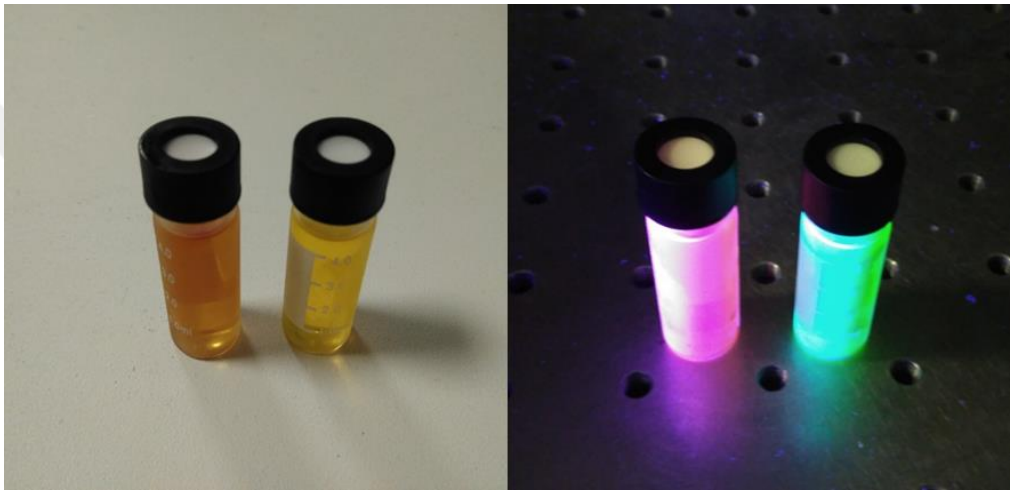

Figure 18: Red and green QD nanocrystals dissolved in Hexane under UV

3.2 Optical Film Fabrication

One of the most crucial aspects among the requirements in preparing high efficient QD film is the efficiency of high color conversation of the QD/polymer film. Because of the accumulation of QDs is nearly associated with the propagation of surface states that enables non-radiative recombination channels, achieving proper spatial distribution of QDs at high concentration in polymer film is an important tread [28, 30]. In order to develop the distribution of QDs in polymer matrix, several methods have been used [31]. Within the film fabrication studies, surface of QDs were functionalized to improve the distribution in QD/polymer films and therefore luminescence efficiency was

increased. Core/shell type CdSe/ZnS QDs and polydimethylsiloxane (PDMS) as a polymer matrix was used for QD/polymer composites.

The fabrication of the QD-polymeric films mainly involves the mixing process of synthesized green- and red-emitting QDs in hexane solvent with Sylgard 184 silicone elastomer (PDMS) and 1.5 g of curing agent in a petri dish by a steel mixer. This process is performed separately for green- and red-emitting QDs. The synthesized QDs were dissolved in Hexane solvent beforehand which simplifies the blending of nanocrystals into the polymer considering the physical difficulty of manipulating the QDs without any supporting material. The relative low boiling temperature of Hexane (at 69°C) promotes the curing process of the polymer and enables the evaporation of the solvent from the QD-polymer mixture.

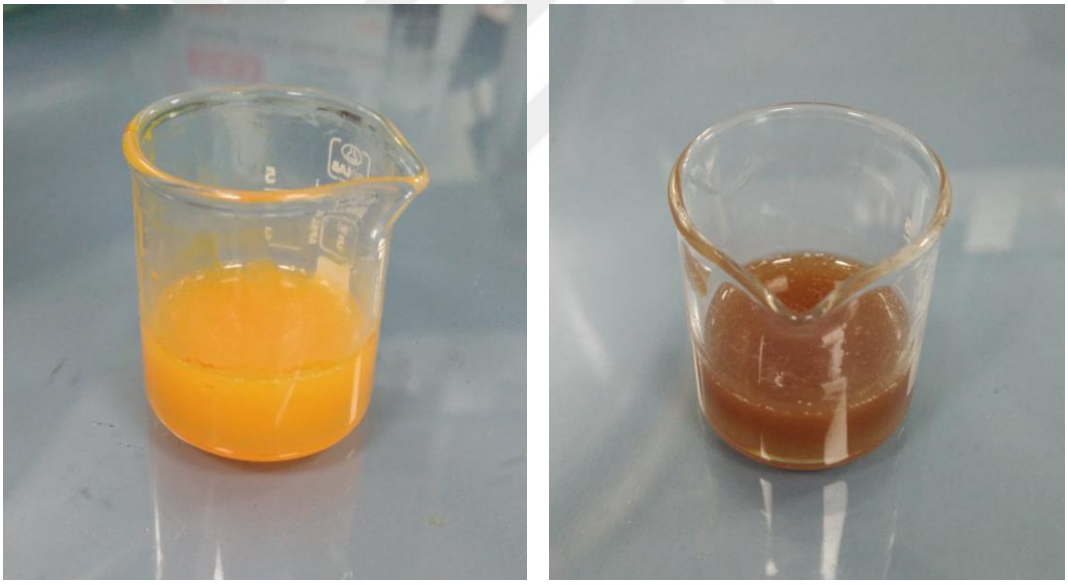

Figure 19: Mixed QD solutions in petri dishes. (left) Green-emitting QD solution and (right) red-emitting QD solution.

Mixed solutions were waited for 30 minutes in vacuum chamber to eliminate atmospheric gas dissolutions that occurred during mixing in order to get smoother solutions. In this way, bubbles and irregularities that could be encountered during the film preparation stage can be prevented.

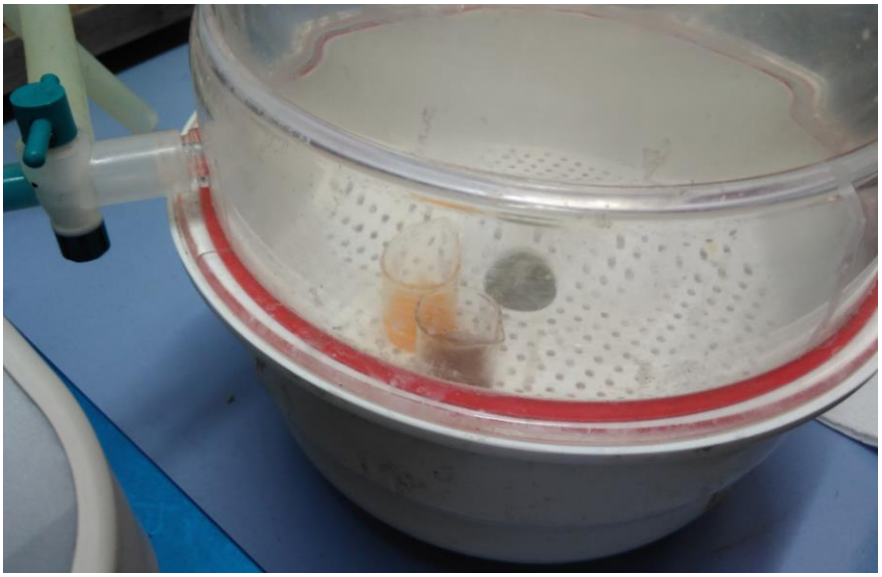

Figure 20: Mixed QDs solutions at vacuum chamber.

Ultra-thin (19 μm thickness) PET film layers were used as barrier films on both sides to prevent the QD film layer from being affected by high oxidation and moisture. In order to produce optical films with desired smoothness and thicknesses, Dr. Blade technique was used on vacuumed table. To achieve a successful application, ultra-thin PET films were placed on the table first. The differences on the surface of the PET films can be seen in Fig. 21 when the vacuuming is off (left) and on (right).

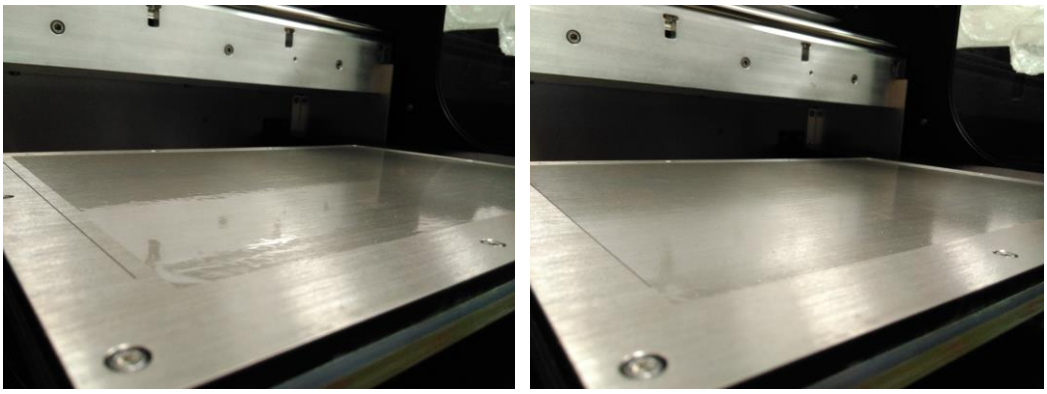

Figure 21: Vacuum table when the vacuuming is (left) off and (right) on.

After the preparation of the application area is completed, vacuumed QD polymer mixture is poured onto the PET film by injection syringe considering the 125 mm x 70 mm smartphone backlight area.

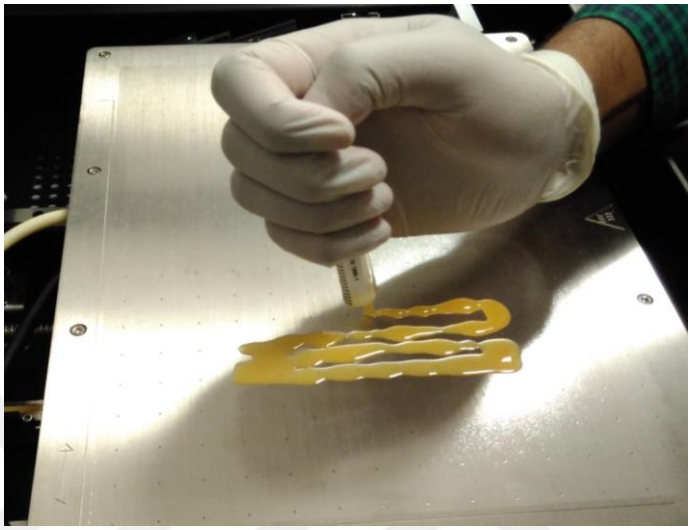

Figure 22: Pouring of the mixture with an injection syringe.

Dr. Blade application was performed with 350 µm applicator thickness for the poured polymer mixture to spread on PET film evenly. Figure 23 shows the green- and red-emitting optical films after the Dr. Blade application.

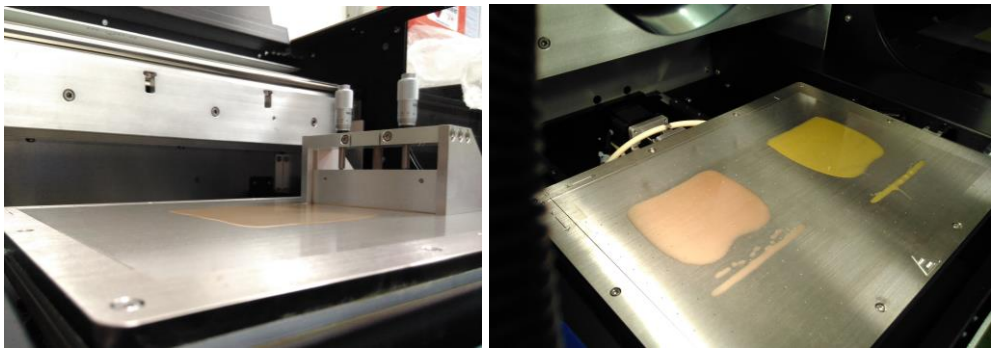

Figure 23: Dr. Blade application.

The final step into the fabrication of QD polymeric films is to heat the products at 90 ºC for 6 hours in a time controlled oven to complete the curing process. Once it is completed, the upper sides of the films were coated with a second PET film which has 19 µm thicknesses as well. Finally, the formed optical films were cut into the 123 mm x 68 mm exact dimensions to be placed in the smartphone BLU.

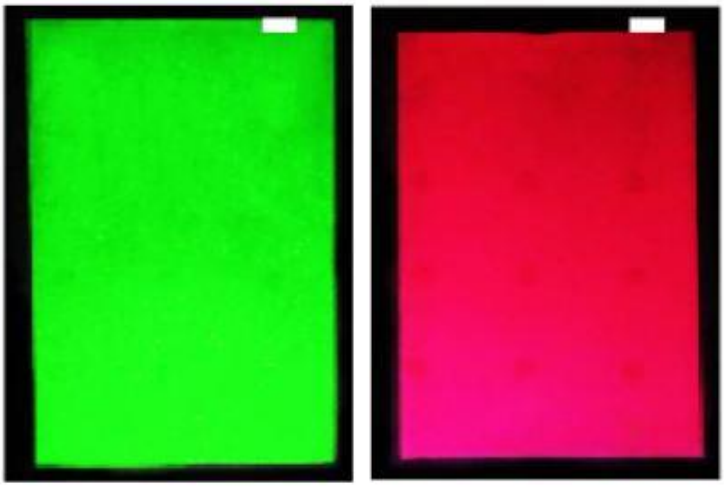

Figure 24: Prepared green- and red-emitted QD films under 365nm UV irradiation.

CHAPTER IV

MEASUREMENTS and RESULTS

4.1 Smartphone Backlight Unit

As stated in Chapter 2, LCDs cannot generate light by themselves, hence they need BLUs for image rendering at visible range. In order to measure the optical measurements of the QD films, the BLU of a smart phone was constructed as shown in Fig 25.

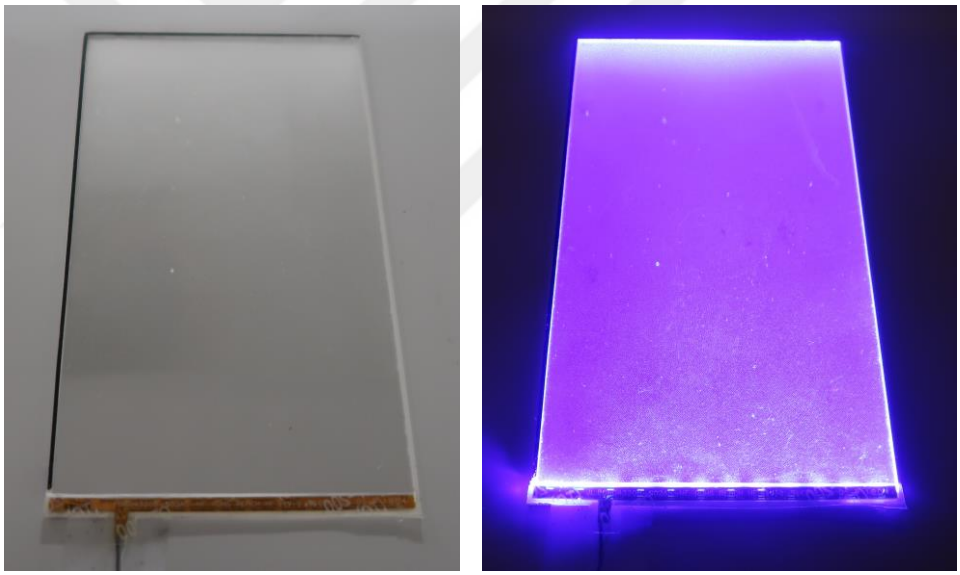

Figure 25: Smartphone BLU (left) off and (right) on.

As a light source, a LED bar with 12 side emitting LED packages was designed with software and produced at Optoelectronic Company as seen in Fig. 26. LED to LED distances on the designed LED bar were determined according to the patterns of the LGP and operated with 100mA driving current.

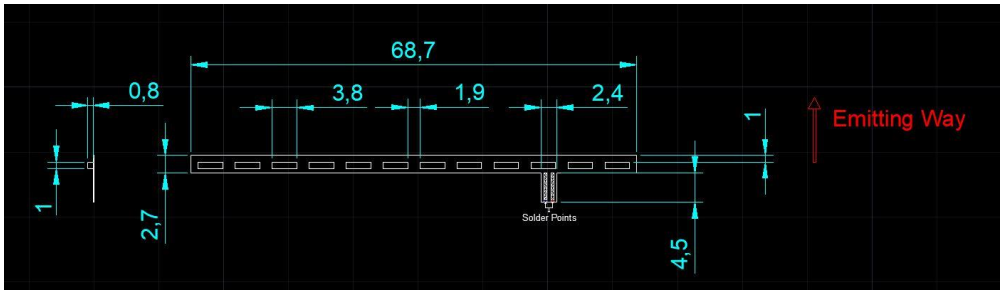

Figure 26: Designed LED Bar 2D drawing.

4.1.1 Optical Structure of Backlight Unit

The optical structure of the BLU was collected using with led bar, light guide plate (LGP), reflector sheet, diffuser sheet, prism sheet and upper diffuser sheet. Schematic optical structure of BLU can be seen in the Fig. 27.

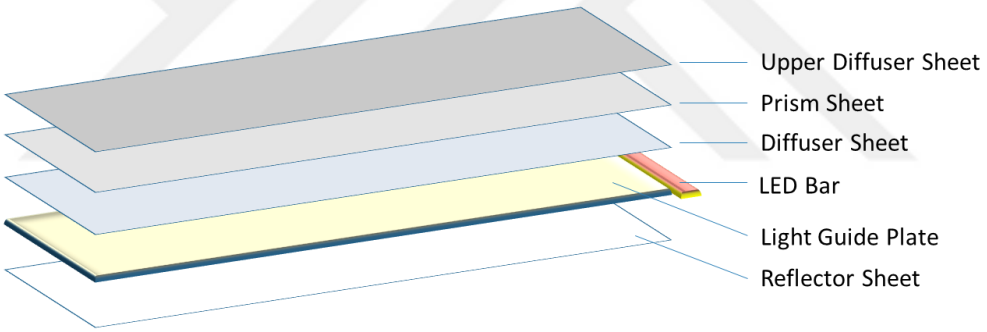

Figure 27: Schematic optical structure of the BLU.

4.2 Color Filter Measurements of the LCD

LCDs form the images on their pixels and each pixel has subpixels containing 3 main color filters. The color filters of each sub-pixel, which are customized as red, green and blue, have a significant transmittance distribution in the visible region. In order to create a display with wide color gamut properties, the transmittance distribution of the color filters and the backlight spectrum must be matched at the dominant peak wavelengths. From this point on, color filter analysis was performed regarding the best color gamut

value with priority.

For the mathematical analysis of the CFA, spectral optical measurements were taken from the LCD screen that is illuminated with white light by BLU using the spectroradiometer as seen in Fig. 28.

Figure 28: Spectroradiometer.

Optical measurements were performed to analyze the light passing through each color filter of the LCD that illuminated by BLU with standard white light source using with spectroradiometer. Thus, intensity measurements at corresponding wavelengths of light passing through each color filter have been made as seen in Fig. 29.

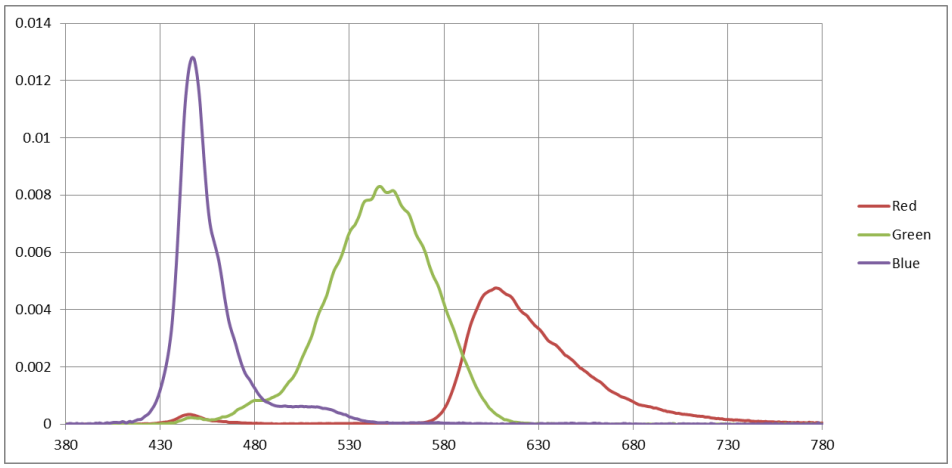

Figure 29: RGB spectral output of the white illuminated LCD.

The spectral distribution of the BLU is also measured by removing the LCD from the panel structure and it is shown in Fig. 30.

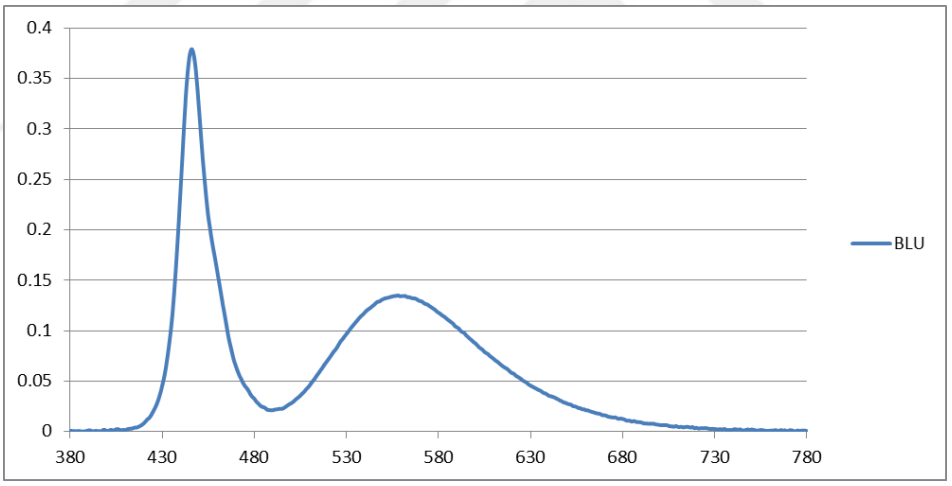

Figure 30: Spectral output of the BLU.

The CFA of the LCD is associated with the distribution of the light from the BLU in the red, green and blue color regions. Transmittance distribution of each color filter can be calculated by dividing the irradiance values of each primary color by irradiance values of the BLU in the wavelength range of 380 to 780 nm.

$$Tr(\%)_{\lambda} = \frac{I_{LCD(\lambda)}}{I_{BLU(\lambda)}} \quad (8)$$

Using with Eq. 8, the transmittance characteristics of the RGB color filters in the wavelength range of 380 and 780 nm was obtained as shown in Fig. 31.

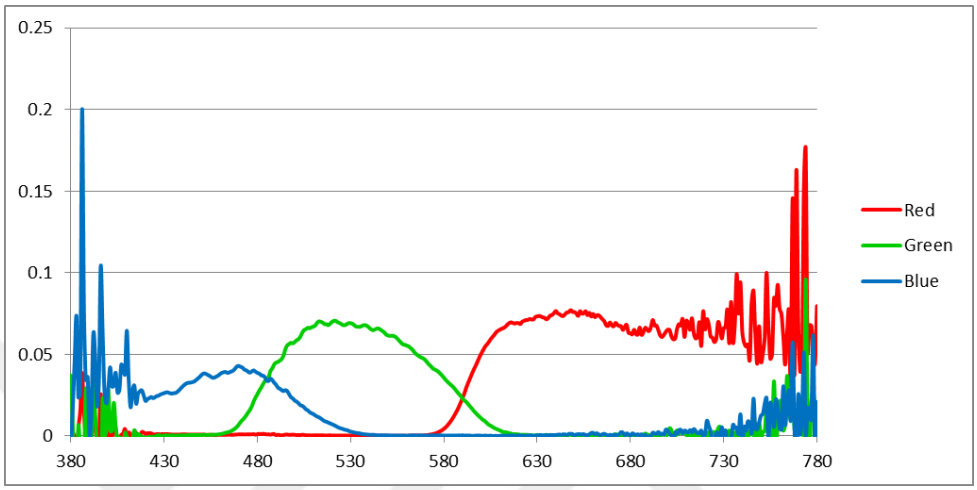

Figure 31: Transmittance characteristics of the RGB CFA.

The luminance, Cx and Cy values were calculated by using spectral irradiance data and the characteristics of the LCD. In this way, the color coordinates and color gamut were calculated preliminary using the mathematical methods before the experimental studies and compared with the measurement results that are shown in Table 1.

Table 1: Cx, Cy and luminance values of BLU and WRGB measurements.

	Cx	Cy	L (nits)
BLU	0.2952	0.2889	7013
Red	0.6254	0.3342	75
Green	0.3220	0.6186	319
Blue	0.1529	0.0475	20
White	0.3179	0.3540	414

In order to calculate average transmittance value of the LCD, the luminance of white color was divided by BLU luminance and calculated as 0.059.

$$Tr_{avg} = \frac{L_{white}}{L_{BLU}} = \frac{414.1\ nits}{7014\ nits} = 0.059$$

4.3 Quantum Dot Measurements

4.3.1 Quantum Dot Photoluminescence Measurements

QDs are luminescent materials that emit light when they are excited by photons. This phenomenon is known as photoluminescence effect of electrons in general [32]. Within the scope of this study, the optical measurement results of synthesized QD nanocrystals which are used during film formation were primarily evaluated by photoluminescence measurements.

UV/Visible absorption and photoluminescence spectra of QDs were measured by Spectroflourometer with 150 W Xenon lamp combined with an excitation monochromator as shown in Fig.32. The excitation wavelength was adjusted to 300 nm with 2 nm FWHM of band pass filter.

Figure 32: Spectroflourometer

The reported optical density, absorbance and photoluminescence spectroscopy measurement was performed by using a standard 1 cm×1 cm quartz cuvette. A single photon counting photomultiplier tube (R928P) was used as emission detector.

4.3.2 Red-Emitting Quantum Dot Photoluminescence Measurements

Emission and absorption spectrums of the red-emitting QDs were measured by the aforementioned methods and shown in Fig. 33 and Fig. 34.

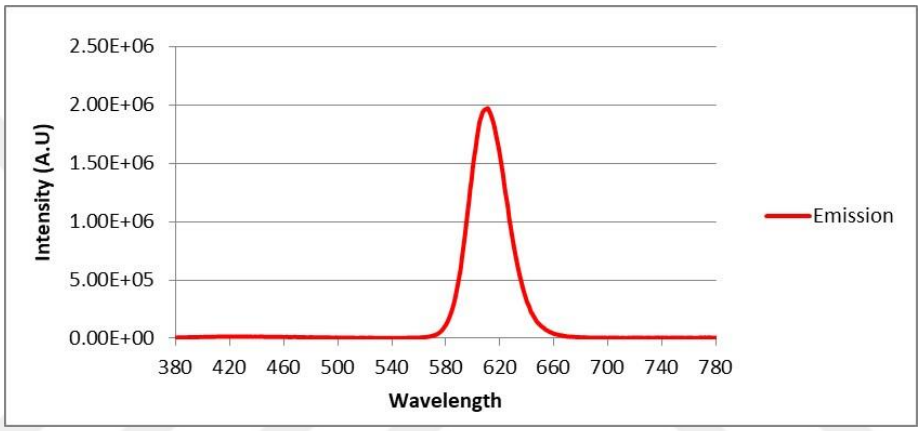

Figure 33: Emission measurement of red-emitting QDs.

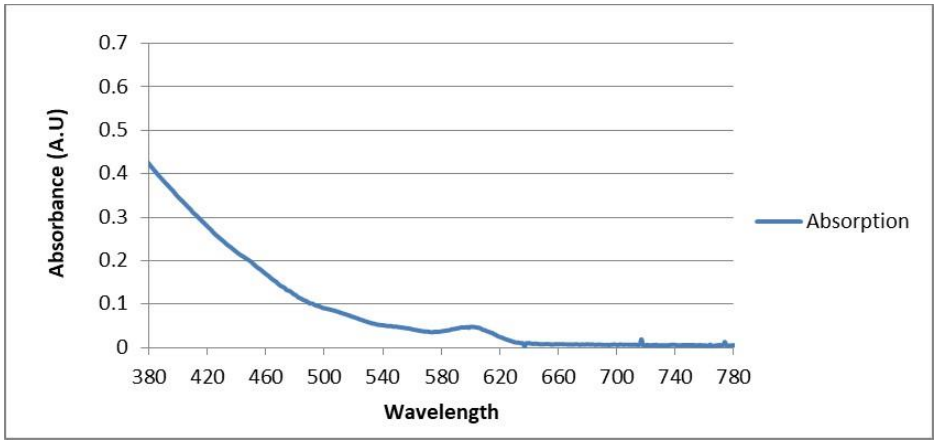

Figure 34: Absorption measurement of red-emitting QDs.

Emission peak wavelength of red-emitting QDs was measured at 620 nm. It is quite satisfactory result when evaluated in terms of the target color gamut and will be

evaluated in more detail at the results section.

4.3.3 Green-Emitting Quantum Dot Photoluminescence Measurements

Emission and absorption spectrums of the green-emitting QDs were measured by using methods that explained at the previous section and shown in Fig. 35 and Fig. 36.

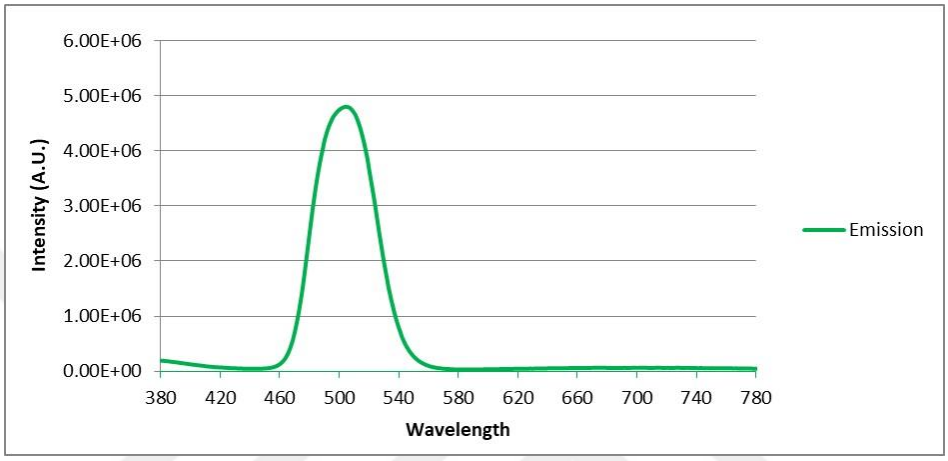

Figure 35: Emission measurement of green-emitting QDs.

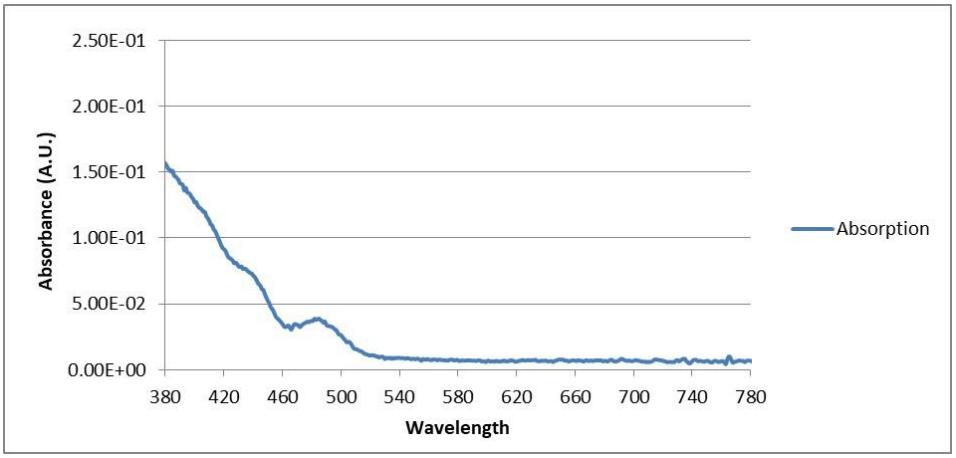

Figure 36: Absorption measurement of green-emitting QDs.

Emission peak wavelength of green-emitting QDs was measured at 510 nm. It is a quite satisfactory result when evaluated in terms of the target color gamut and will be evaluated in more detail at the results section.

4.4 Quantum Dot Film Measurements

In order to perform optical measurements, LED packages with InGaN / GaN chip structure were used as light source on LED bar which produced at Optoelectronics Company. BLU spectral measurements were performed using optical spectroradiometer shown in Fig 28. Produced films were placed in the BLU structure with the film combination as shown in Fig. 37. The measuring device included in the schematic drawing was placed at a distance of 10 mm for the optical measurements.

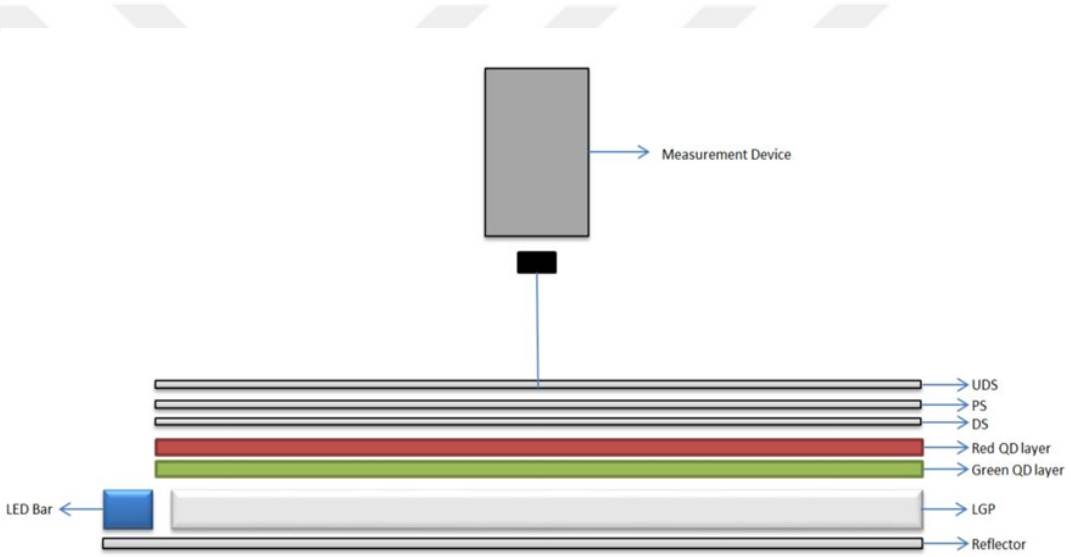

Figure 37: Structural optical film combination of BLU.

4.4.1 Optical Analysis of Produced QD Films

To evaluate the optical performance of produced red- and green-emitting QD films, synthesized QDs and PDMS polymer were fabricated at same concentration and different thicknesses from 100 µm to 500 µm using with Dr. Blade technique as shown in Fig. 38.

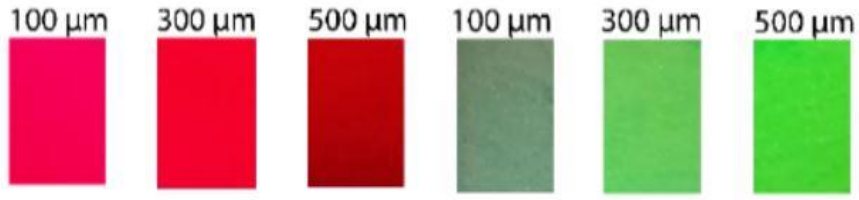

Figure 38: Produced red- and- green-emitting QD films with different thicknesses

In order to observe brightness improvement on QD films, film thicknesses were increased from 100 µm to 500 µm. With the increase of film thicknesses, it was observed that the brightness of the films is enhanced when they are irradiated under 365 nm UV light. At the same time, QD films were irradiated by the blue LEDs which are used at the BLU structure and measured with spectroradiometer. As a result of spectral measurements, it was observed that blue light intensity decreases when the QD film thicknesses are increased, because the color conversion ratio is higher at thicker QD films as seen in Fig. 39.

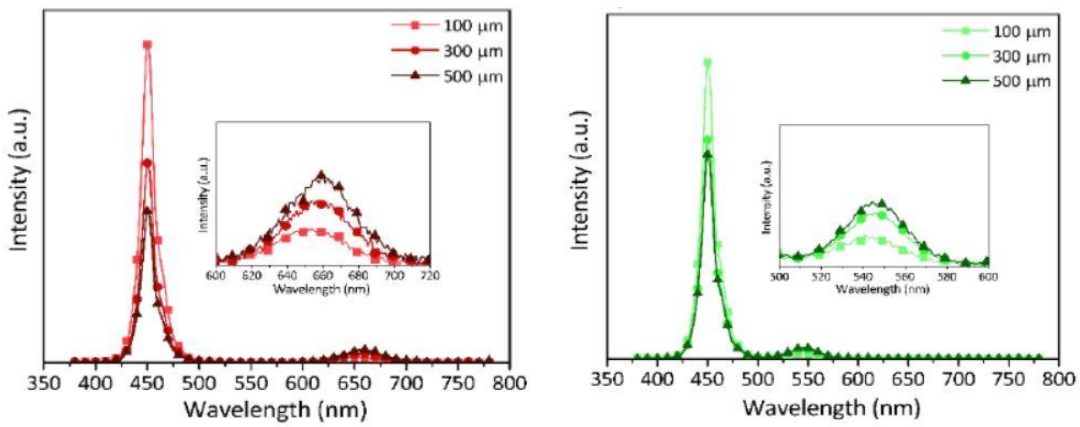

Figure 39: The optical intensity output of the fabricated red- and green-emitting films with different thicknesses when excited by blue source

4.4.2 Red-Emitting CdSe/CdS & Green-Emitting CdSe/ZnS QD Film Measurements at LCD Panel

Red- and green-emitting QD films were produced with 1 ml nanocrystalline solution and mixture of 4.5 g of polymer using the synthesis and film forming methods mentioned in Chapter 3.

The spectrum of BLU with an optical structure that involves the red-emitting CdSe/CdS and green-emitting CdSe/ZnS QD films are shown in Fig 40.

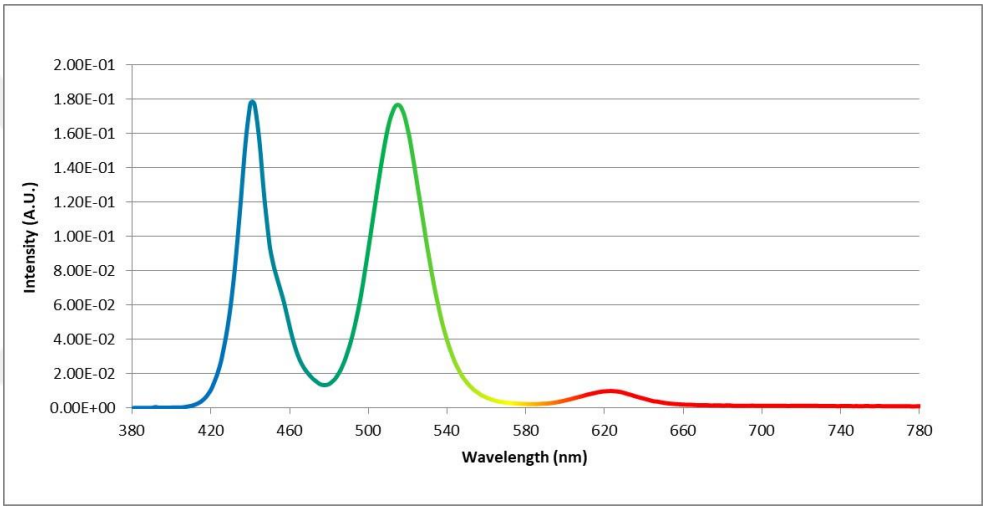

Figure 40: Spectrum output of the red-emitting CdSe/CdS and green-emitting CdSe/ZnS QD films in the BLU.

Luminance, Cx and Cy values were calculated using spectrum raw data and previously calculated color filter data. The results obtained from the calculations are summarized in Table 2.

Table 2: Optical outputs of red-emitting CdSe/CdS and green-emitting CdSe/ZnS QD films in the LCD.

	Cx	Cy	L (nits)
BLU	0.1561	0.2939	2791
Red	0.5454	0.2829	8
Green	0.1071	0.7209	172
Blue	0.1391	0.1148	25
White	0.1465	0.4246	205

The color gamut value was calculated as **80** % according to the NTSC standard in CIE 1931 color space by using Cx & Cy values of RGB colors as shown in Fig. 41.

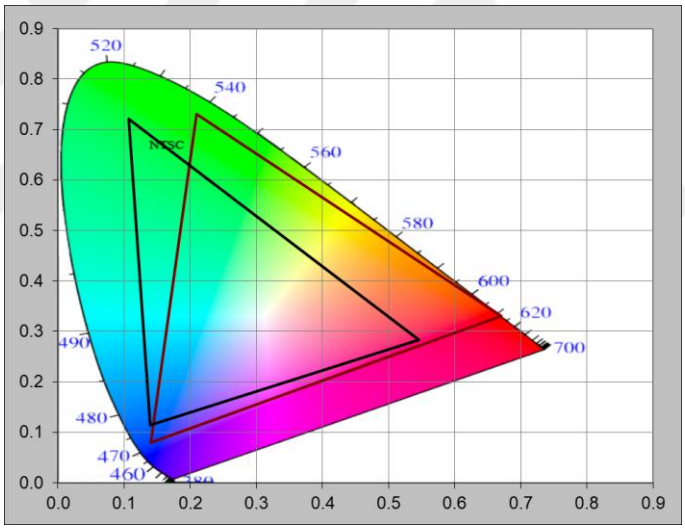

Figure 41: Color gamut triangle of the red-emitting CdSe/CdS and green-emitting CdSe/ZnS QD films in the LCD.

4.4.3 Red-Emitting CdSe/ZnS & Green-Emitting CdSe/ZnS QD Film Measurements at LCD Panel

Red and green QD films were produced with 1 ml nanocrystal solution and mixture of 4.5 g of polymer using the synthesis and the aforementioned film forming methods.

Produced films were placed in the BLU with the film combination shown in Fig. 37, and measurements were made. The spectral results are shown in Fig. 42.

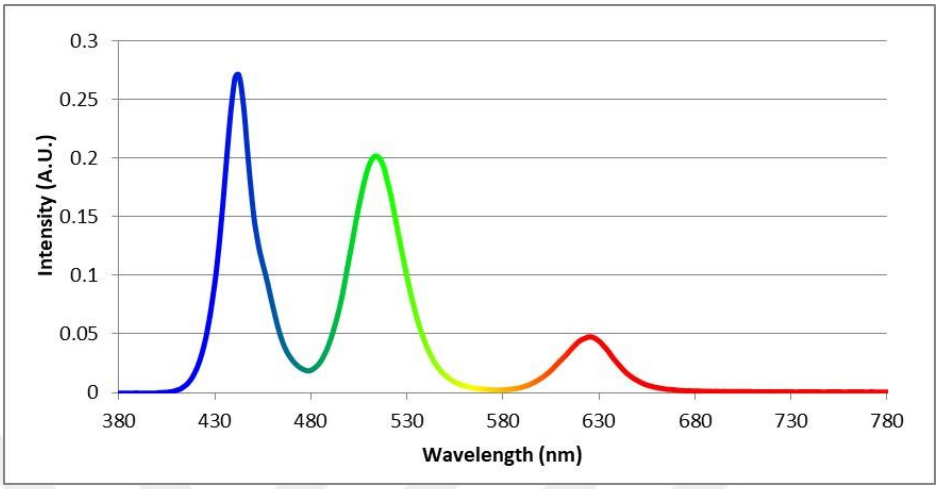

Figure 42: Spectrum output of the red-emitting CdSe/ZnS and green-emitting CdSe/ZnS QD films in the BLU.

Luminance, Cx and Cy values were calculated using spectrum raw data and previously calculated color filter data. The results obtained from the calculations are summarized in Table 3.

Table 3: Optical outputs of red-emitting CdSe/ZnS and green-emitting CdSe/ZnS QD films in the LCD.

	Cx	Cy	L (nits)
BLU	0.1903	0.2449	3446
Red	0.6276	0.2960	28
Green	0.1081	0.7043	192
Blue	0.1431	0.0942	31
White	0.1963	0.3621	251

The color gamut value was calculated as **95.7** % according to the NTSC standard in CIE 1931 color space by using Cx & Cy values of RGB colors as shown in Fig. 43.

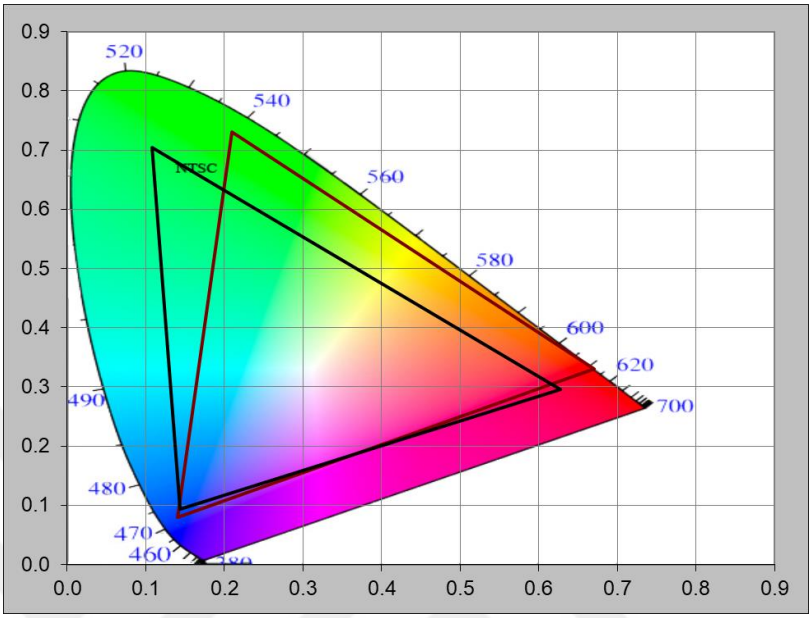

Figure 43: Color gamut triangle of the red-emitting CdSe/ZnS and green-emitting CdSe/ZnS QD films in the LCD.

4.5 Discussion

The experimental data corresponding to optical performance of the synthesized QD nanocrystals reveals significant outcomes. The most noteworthy part in terms of optical outputs is the increment of the color gamut value when the blue LED + QD film layer used as BLU. While the color gamut of the BLU with a standard white LED structure is 70%, we have reached 95% value with the QD film solution. The schematic improvement in the color gamut triangle is seen in Fig. 44.

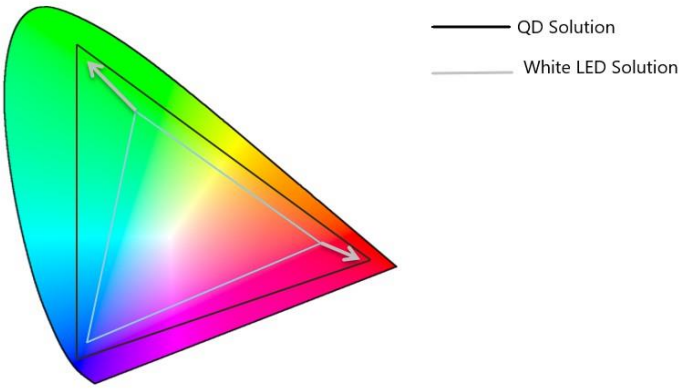

Figure 44: Schematic improvement in the color gamut triangle

The change in the corner points of the triangle in red and green color regions provided 35% gain in color gamut of produced display. The difference in color quality between the displays that consists the produced QD-films and the commercial product can be clearly distinguished shown in Fig. 45. The commercial product is on the left and the product containing QD-film is on the right.

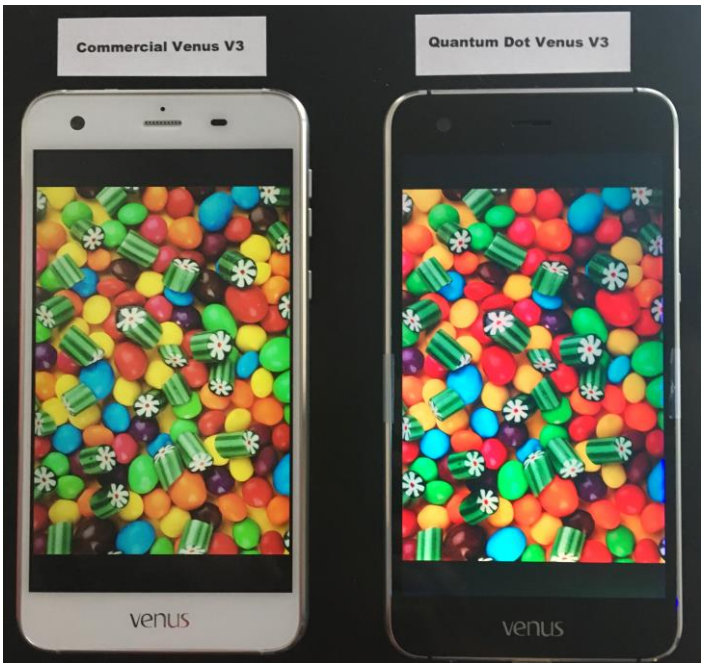

Figure 45: Color quality difference of the produced displays. (left) Commercial product contains standard white LED in BLU, (right) QD film embedded product.

Despite the fact that QD based films involve green- and red-emitting QDs together in large size displays; smartphone size films manifest red color dominancy. The absorption spectrum of the red-emitting QDs also involves the green region, as shown in Fig. 34; hence green emitted photons are reabsorbed by the red-emitting QDs with dramatic decrease in the amount of green-emitted photons. The concentration levels can be arranged in large size panels such that the effect of reabsorption can be reduced. However, in small size films, concentration levels cannot be increased too much because of the agglomeration of QD nanoparticles. Therefore, green- and red-emitting QDs are used separately in this study.

The order of the films is determined according to the experimental data as well. When the red-emitting film is placed under the green-emitting film, it absorbs most of the blue photons, therefore decreases the emission level of the green QDs dramatically. When the positions of the films are swapped, the effect of the green QDs is increased.

CHAPTER V

CONCLUSION

Within the scope of this thesis study, the color gamut of the smartphone display was increased by 35% relative to the NTSC standard by means of QD optical films adapted BLU.

Initially, QDs with CdSe core structure were synthesized for yielding emission peaks at green and red regions of the visible spectrum. The emission and absorption spectra of the synthesized particles were analyzed and most suitable particle types and sizes, consequently most suitable FWHM and peak wavelengths were determined in order to increase the color gamut of the smartphone display. The CdSe / ZnS particle structure was used as QDs due to the high quantum efficiency, having peak wavelength of 620 nm for red color and 510 nm for green color and 40 nm of FWHM. Optical films were encapsulated within PDMS polymer and molded by Dr. Blade method at different mixing ratios. During the film preparation process, different concentrations and thicknesses were produced and their optical performances were compared to determine the optimal particle concentration and film thickness in accordance with smartphone BLU dimensions. Separate films were produced as green- and red-emitting QD layers and corresponding optical measurements of the final products resulted as 95.7% NTSC color gamut in CIE 1931 standard.

Experimental studies have been published in Materials Research Express in 2019 under the name of "High quality quantum dots polymeric film converters for smart phone display technology".

BIBLIOGRAPHY

[1] M. Schadt, “Milestone in the history of field-effect liquid crystal displays and materials,” Journal of Applied Physics 48, No: 3, 03B001, (2009).

[2] K. M. Chen et al., “Sub millisecond gray level response time of polymer-stabilized blue-phase liquid crystal,” Journal of Display Technol. 6, No: 2, 49-51, (2010).

[3] J. Cho, J. H. Park, J. K. Kim, E.F. Schubert, “White light-emitting diodes: History, progress, and future”, Laser Photonics Rev. 11, No: 2, 1600147 (2017).

[4] Y. Shirasaki, G. J. Supran, M. G. Bawendi, V. Bulovic, “Emergence of colloidal quantum-dot light-emitting technologies” Nature Photonics, Vol 7, DOI:10.1038/NPHOTON.2012.328, (2013).

[5] G. Wyszecki, WS. Stiles, “Color science: concepts and methods, quantitative data and formulae”, NY: Wiley-Interscience; (2000).

[6] Webvision, The Organization of the Retina and Visual System, (Accessed Dec 26, 2018, at http://webvision.med.utah.edu/book/part-i-foundations/simple-anatomy-of-the-retina/).

[7] Schubert EF., “Light-emitting diodes”, New York: Cambridge University Press, (2006).

[8] CIE Commission Internationale de l’Éclairage Proceedings, Cambridge: Cambridge University Press, (1932).

[9] Harris A. C., Weatherall I. L., "Objective evaluation of color variation in the sand-burrowing beetle Chaerodes trachyscelides White (Coleoptera: Tenebrionidae) by

instrumental determination of CIE LAB values", Journal of the Royal Society of New Zealand, 20 (3): 253–259, (1990).

[10] Castellano JA., “Handbook of Display Technology”, Amsterdam, the Netherlands: Elsevier, (2012).

[11] Yeh P., Gu C., “Optics of Liquid Crystal Displays”, New York, USA: John Wiley & Sons, (2010).

[12] Yang DK, Wu ST., “Fundamentals of Liquid Crystal Devices”, 2nd edn, New York, USA: John Wiley & Sons, (2014).

[13] M. Anandan, “LCD backlighting”, Society for Informational Display Seminar Lecture Notes, pp. 169–250, (2002).

[14] H. Chen, J. He, S.T. Wu, “Recent Advances on Quantum-Dot-Enhanced Liquid-Crystal Displays”, IEEE Journal of Selected Topics in Quantum Electronics, VOL. 23, No: 5, (2017).

[15] J. Souk, S. Morozumi, F.C. Luo, I. Bita, “Flat Panel Display Manufacturing”, John Wiley & Sons, (2018).

[16] G. Lee, J. H. Jeong, S. J. Yoon, D. H. Choi, “Design optimization for optical patterns in a light-guide panel to improve illuminance and uniformity of the liquid-crystal display”, Opt. Eng., 48(2), p. 024001, (2009).

[17] W. G. Lee, J. H. Jeong, J. Y. Lee, K. B. Nahm, J. H. Ko, J. H. Kim, “Light Output Characteristics of Rounded Prism Films in the Backlight Unit for Liquid Crystal Display”, J. of Information Display, 7(4), p. 1 (2006).

[18] T. Erdem, H.V. Demir, “Color science of nanocrystal quantum dots for lighting and displays”, Nanophotonics, (1):57-81, (2013).

[19] Koole R., “Fundamentals and applications of semiconductor nanocrystals: a study on the synthesis, optical properties, and interactions of quantum dots”, PhD Thesis, Netherlands: Utrecht University; (2008).

[20] Bera D., Qian L., Holloway P.H., “Semiconducting quantum dots for bioimaging. In: Pathak Y, Thassu D, editors. Drug delivery nanoparticles formulation and characterization”. London, UK: Informa Healthcare,349– 66, (2009).

[21] Gaponik N., Hickey S.G., Dorfs D., Rogach A.L., “Progress in the light emission of colloidal semiconductor nanocrystals”, Small;6:1364– 78, (2010).

[22] Reiss P., Proti è re M, Li L., “Core/shell semiconductor nanocrystals”, Small; 5:154– 68 (2009).

[23] Jang E., Jun S., Jang H., Lim J., Kim B., Kim Y., “White-light-emitting diodes with quantum dot color converters for display backlights”, Adv Mater, 22:3076 – 80, (2010).

[24] Fu, Y., et al., Excellent stability of thicker shell CdSe@ ZnS/ZnS quantum dots. RSC Advances, 2017. 7(65): p. 40866-40872.

[25] Bahmani Jalali, H., et al., Excitonic Energy Transfer within InP/ZnS Quantum Dot Langmuir–Blodgett Assemblies. The Journal of Physical Chemistry C, 2018. 122(22): p. 11616-11622.

[26] Lim J., et al., “Preparation of highly luminescent nanocrystals and their application to light-emitting diodes”, Advanced Materials, 19(15): p. 1927-1932, (2007).

[27] Bae W.K., et al., “Highly Efficient Green-Light-Emitting Diodes Based on CdSe@ ZnS Quantum Dots with a Chemical-Composition Gradient”, Advanced Materials,. 21(17): p. 1690-1694, (2009).

[28] X.D. Cao, C.M. Li, H.F. Bao, Q.L. Bao, H. Dong, “Fabrication of strongly fluorescent quantum dot–polymer composite in aqueous solution”, Chem. Mater. 19 3773–3779, (2007).

[29] M. Noh, T. Kim, H. Lee, C.K. Kim, S.W. Joo, K. Lee, “Fluorescence quenching caused by aggregation of water-soluble CdSe quantum dots”, Colloid Surf. A 359 39–44, (2010).

[30] C.W. Wang, M.G. Moffitt, “Surface-tunable photoluminescence from block copolymer-stabilized cadmium sulfide quantum dots”, Langmuir, 20 11784–11796, (2004).

[31] M. Zorn, W.K. Bae, J. Kwak, H. Lee, C. Lee, R. Zentel, K. Char, “Quantum dot–block copolymer hybrids with improved properties and their application to quantum dot light-emitting devices”, ACS Nano 3 1063–1068, (2009).

[32] K.N. Dhoble, S.J. Swart, H.C. Park, “Phosphate Phosphors for Solid-State Lighting”, ISBN: 978-3-642-34311-7, (2012).

VITA

Süleyman Efdal Mutcu was born in 1990, in Isparta, Turkey. He has received his BSc degree from Physics Engineering Department of Hacettepe University in 2014. He has been working at VESTEL Electronics Corp. as Senior Optical System Design Engineer since 2015. His current research interests are display systems, optical design of backlight systems, new display technologies and quantum dots.